Heliyon 10 (2024) e32880

Contents lists available at ScienceDirect

Heliyon

journal homepage: www.cell.com/heliyon

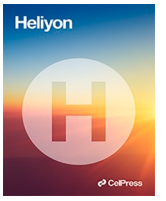

Research article

Soil erosion assessment and identification of erosion hotspot areas in the upper Tekeze Basin, Northern Ethiopia

Alemu Eshetu Fentaw [a,b,*], Assefa Abegaz [a]

[a] Department of Geography and Environmental Studies, Addis Ababa University, Addis Ababa, Ethiopia
[b] Department of Geography and Environmental Studies, Woldia University, Woldia, Ethiopia

ARTICLE INFO

Keywords:
Revised universal soil loss equation
Google earth engine land use
Agroecologies
Land management
Upper Tekeze basin
Waghimra administrative zone

ABSTRACT

Soil erosion is a major environmental problem in Ethiopia, reducing topsoil and agricultural land productivity. Soil loss estimation is a critical component of sustainable land management practices because it provides important information about soil erosion hotspot areas and prioritizes areas that require immediate management interventions. This study integrates the Revised Universal Soil Loss Equation (RUSLE) with Google Earth Engine (GEE) to estimate soil erosion rates and map soil erosion in the Upper Tekeze Basin, Northern Ethiopia. SoilGrids250 m, CHIRPS-V2, SRTM-V3, MERIT Hydrograph, NDVI from sentinel collections and land use land cover (LULC) data were accessed and processed in the GEE Platform. LULC was classified using Random forest (RF) classification algorithm in the GEE platform. Landsat surface reflectance images from Landsat 8 Operational land imager (OLI) sensors (2021) was used for LULC classification. Besides, different auxiliary data were utilized to improve the classification accuracy. Using the RUSLE-GEE framework, we analyzed the soil loss rate in different agroecologies and LULC types in the upper Tekeze basin in Waghimra zone. The results showed that the average soil loss rate in the Upper Tekeze basin is 25.5 t ha^{-1} yr^{-1}. About 63 % of the basin is experiencing soil erosion above the maximum tolerable rate, which should be targeted for land management interventions. Specifically, 55 % of the study area, which is covered by unprotected shrubland is experiencing mean annual soil loss of 34.75 t ha^{-1} yr^{-1} indicating the need for immediate soil conservation intervention. The study also revealed evidence that this high mean soil loss rate of the basin can be reduced to a tolerable rate by implementing integrative watershed management and exclosures. Furthermore, this study demonstrated that GEE could be a good source of datasets and a computing platform for RUSLE, in particular for data scarce semi-arid and arid environments. The results from this study are reliable for decision-making for rapid soil erosion assessment and intervention prioritization.

1. Introduction

Almost all over the world, water availability, biodiversity, and agricultural productivity are threatened by land degradation processes [1–4]. Although land degradation has many components and definitions, in ecological perspectives, it includes several processes that may cause biodiversity loss and a decline in ecosystem functions and services [5]. Soil erosion by water is among the primary forms of land degradation, causing grave environmental problems and food insecurity [6,7]. It decreases soil mass, depletes

* Corresponding author.
E-mail addresses: eshetualemu.ae@gmail.com (A.E. Fentaw), assefa.abegaz@gmail.com (A. Abegaz).

https://doi.org/10.1016/j.heliyon.2024.e32880
Received 27 July 2023; Received in revised form 10 June 2024; Accepted 11 June 2024
Available online 13 June 2024

soil nutrients, and increases down-stream river sedimentation and siltation of reservoirs [6,8]. In sub-Saharan Africa, especially in East Africa, with its degraded complex topography accompanied with high rainfall intensity; soil erosion and nutrient depletion threaten food security and sustainable agricultural production [9–12]. Although it seems very difficult to establish the exact time when soil erosion in the history of agriculture was considered a problem in Ethiopia, many soil and water conservation interventions were introduced following the rising global awareness of land degradation and after the severe drought of Ethiopia in 1974 [13–15]. Nevertheless, soil erosion is still a significant challenge in Ethiopia [13,16,17], particularly in the country's highlands due to high rainfall erosivity, intensive agricultural practices, and high population pressure [18,19]. Northern dry land areas of Ethiopia are more susceptible to soil erosion because their ecology is considerably damaged attributed to easily degradable soils, highly variable temperature and rainfall, cultivation on steep slopes, deforestation, and dense and rapidly growing economically marginalized populations [4]. As a result, the country's backbone of the economy, agriculture, is severely affected by persistent soil erosion in the northern highlands of Ethiopia [14,20]. It has been suggested that soil erosion in this area could be worsen because of increased population and predicted rise in precipitation [13,21]. The country has implemented short- and long-term plans to reverse and minimize land degradation through different community-based strategies. Both in its Growth and Transformation plan (GTP) and Climate Resilient Green Economy (CRGE), the Ethiopian government adopted strategies to address the effects of land degradation caused by soil erosion and build a climate-resilient green economy by 2025 [22–24]. However, given the economic and technical limitations to the conservation of all areas affected by soil erosion, targeting areas with high soil loss rates is required for effective and proper allocation of limited resources [13,22,25]. For this purpose, scientifically investigated, organized, and mapped soil erosion severity status, at a basin-level, is prerequisite to identify priority areas of conservation.

In Ethiopia, there are regional differences regarding efforts made to understand soil erosion processes [13]. For example, Tekeze basin located in the Tigray highlands was among the major basins of Ethiopia that has got much attention from researchers. However, most of the previous studies were plot-scale, or small-scale at small-watershed; and were fragmented. Recently, majority of the sub-basin and basin-based soil erosion assessments studies are conducted in Blue Nile Basin [26–31], and Rift Valley Basin [17,32–36], while data on soil erosion status in the Tekeze River basin in Waghimra administrative zone is scarce. Since the basin is home to millions of rural farmers whose economy mainly depends on rain-fed agriculture, estimating soil erosion rates and identifying erosion hotspot areas at basin level is critical for land and water resource management. Moreover, this basin is ecologically and historically vulnerable to soil erosion due to degraded forest cover, high population pressure, and complex topography that aggravate soil erosion.

According to Karydas et al. [37] more than 80 erosion models have been developed for different purposes in half a century. Among those models, Universal Soil Loss Equation (USLE, [38]), Modified Universal Soil Loss Equation (MUSLE, [39]), European Soil Erosion Model (EUROSEM, [40]), and Water Erosion Prediction Project (WEPP, [41]) are commonly preferred by researcher around the world. Above all, USLE and its revised version; Revised Universal Soil Loss Equation (RUSLE [42]) are the most frequently used models in soil erosion studies [43,44]. RUSLE is used to estimate annual average soil loss rate by accounting for rainfall erosivity, soil erodibility, slope, land use, and land management attributes [38,42]. Since soil erosion assessment as well as sustainable land and water management are increasingly requiring big-data-driven policymaking and management strategies; Remote sensing (RS) and Geographic Information System (GIS) tools are facilitating the development of soil erosion models [45–47]. However, RS and GIS based soil erosion models require extensive field soil data collection, which is expensive and time-consuming constraining soil erosion assessment for present priority use. Furthermore, the increasingly available high-resolution gridded soil and other vegetation-related data are not well utilized to estimate soil loss rates [27].

Google Earth Engine (GEE) has recently become a popular cloud-computing platform for retrieving and analyzing geospatial data [48,49]. GEE offers cutting-edge technologies and unrestricted access to various remote sensing data, fostering the formation of transformative research issues. GEE has been used for a variety of applications, such as drought assessment [50,51] and land use-land cover change (LULCC) and vegetation mapping [52–54]. However, there are very few attempts to estimate soil loss estimation through the RUSLE-GIS-GEE framework by integrating ArcGIS and GEE interface [55], for example, studies by Elnashar et al. [56] and Wang and Zhao [57]. Implementing RUSLE in the GEE environment minimizes data filtering and image correction time. It facilitates accurate estimation of soil erosion at global, regional, and watershed scales by increasing readily available soil, precipitation, and topographic variables [56]. Using common datasets in the GEE could also help produce comparable results among different studies by minimizing data-related errors and uncertainties. The increasing availability of open data sources, for example, Multi-Error-Removed Improved-Terrain (MERIT) Hydrograph, SoilGrids250 m, and high-resolution sentinel images in GEE have also increased the suitability of this cloud-based platform for soil erosion studies. Particularly time-series data management for Normalized difference vegetation index (NDVI) and spatio-temporal rainfall analysis could be much easier in the GEE environment. Furthermore, integrating the classification algorithm, primarily the Random forest (RF) algorithm, could improve land cover classification for RUSLE.

Methodologically, this study aims to contribute to soil erosion assessment based on RUSLE- GEE framework. In addition, the study applied the upslope contributing area approach in order to derive the slope length (L) factor. This approach is more appropriate in basin-based studies because the upstream contributing area is a more determinate factor than slope length in those areas [25,44,58]. In addition, most of the available studies in Ethiopia used LULC as a proxy measurement for the C-factor. However, in semi-arid and arid land areas, land cover classification is complicated due to the similarity of reflectance from the different LULCs. In these cases, NDVI is decisive in differentiating surface reflectance. Furthermore, the current study fills the gap in the LULC classification system by implementing random forest (RF) algorithm and adding 5 Axillary data (NDVI, Normalized difference witness index (NDWI), Tesseled Cap indices, slope and elevation) to achieve higher accuracy.

Therefore, the overall objective of this study was to provide an up-to-date basin level soil loss severity map and implication of estimated soil loss severity for suitable land management practices in the upper Tekeze basin using RUSLE–GEE framework. The specific objectives were to: 1) estimate and map the extent and severity of soil loss by water erosion in the Upper Tekeze Basin, 2)

analyse soil loss estimates in relation to land cover types and agroecological zones of the basin, and 3) identify soil erosion hotspot areas of the basin for watershed management interventions.

Since land management practices depend on land cover types and agroecology [22], the result from this study can solve the scarcity of soil loss data as well as help land degradation control and land resources management practices by raising awareness among policy makers and land managers on the extent and severity of soil loss by water erosion. The result could also serve as feedback for the long-term conservation works implemented in the basin over the past three decades.

2. Methods and datasets

2.1. Study area description

Tekeze River is one of the major tributaries of the Nile River. The river originates from the highlands of North Wollo, from Mount Abune Yosef, drains to Waghimra, Tigray, and finally enters Sudan to join the Nile River. Tekeze river basin is situated in the north-western part of Ethiopia and forms the most northern part of the Nile Basin within Ethiopia. The basin covers about 66,541 km^2, extends from 35.87° to 39.87° East, and 11.52°–14.8° North [59]. The basin is surrounded by the Blue Nile (Abay), Angereb and Mereb Rivers, and the Afar Rift escarpment. The current study is conducted on the river's upper basin in Waghimra Administrative Zone. Geographically the study area extends from 12.11 to 13.13^0 N latitude and 38.40^0 to 39.30^0 E longitude (Fig. 1). The study area includes 4 rural administrative districts in Waghimra zone, namely Gazgibla, Sekota Zurya, Zquala, and Tsagbji. In this part of the basin, there exists very diverse and rugged topography. While the altitude of Tekeze basin in Ethiopia ranges from 500 m in its western lowlands to over 4600 m in the central highlands, in the current study district, the elevations range from 1021 to 3880 m above sea level (Fig. 1). Based on Hurni's [60] agroecological classification which considers elevation, three different agroecological zones dominate the study area. The Kolla agroecological zone (warm, semiarid lowlands; covering 17.5 %), followed by Weyna-dega (cool, humid highlands; covering 68 %), and Dega (temperate cool sub-humid highlands; covering 14.5 % of the study area). Most of the study area is semi-arid and arid according to the United Nations Environment Programme (UNEP) aridity classification [51]. While the northern and northeastern part of the basin is dry sub-humid and non-dryland, the central and northern holds semi-arid and arid land characteristics.

Unimodal and erratic rainfall patterns characterize rainfall in Waghimra zone. The basin receives much of its annual rainfall from June to September (locally known as "*Kiremt*") when the Inter Tropical Convergence Zone (ITCZ) is located north of Ethiopia [61]. This rainy season contributes over 70 % of the annual precipitation in north and northwest Ethiopia, including in the Waghimra zone. While the annual rainfall of the Tekeze basin reaches up to 2000 mm in the Ras Dashen Mountains [61], it is less than 1000 mm in the upper river basin in the Waghimra administrative zone (Fig. 2).

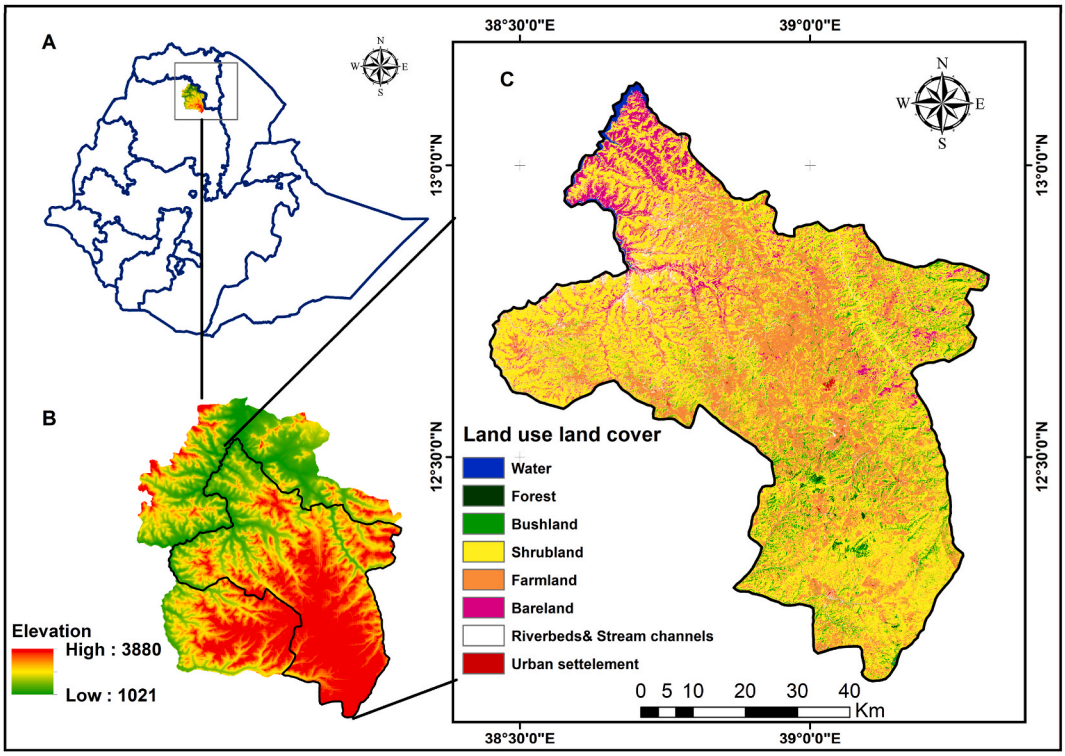

Fig. 1. Location of the study area: a) in Ethiopia, b) in Waghimra Adminstrative Zone c) studied sub-basin showing land use land cover.

In almost all parts of the Tekeze basin, the summer (*Kiremt)* rain ceases around the end of August. The mid and high-altitude areas receive rainfall from late June to early September. However, rainfall distribution of the lowland part extends from early July to mid of August. About 63 % of the annual rainfall is in July and August [51]. The area's annual minimum and maximum temperatures are 12.8 °C and 29 °C, respectively (Fig. 2). The primary crop production system is based on the summer season.

Over 90 percent of households throughout the Wag-himra Zone live on smallholder farming with landholdings of less than 1 ha. The agricultural activities are rain-fed, with the main harvest from September to November. Farmers produce mainly cereals (sorghum, teff, barley, and wheat), pulses, and vegetables. The region is characterized by severe land degradation, climate variability, and high population density [62]. The zone has been one of the most drought-affected areas in the past. High vulnerability to drought and famine, growing population pressure, and land degradation have affected agricultural production.

2.2. Datasets

Data used in this study includes i) Climate Hazards Group InfraRed Precipitation with Station data (CHIRPS) precipitation, ii) SoilGrids data, iii) LULC data, iv) NDVI, and v) Shuttle Radar Topographic Mission (SRTM) Digital Elevation Model (DEM). The general overview of flow of the methology applied to assess soil erosion by water in RUSLE–GEE framework is depicted on Fig. 3. Detailed description of the different data used in the study is presented in the following subsections.

2.2.1. Precipitation data

CHIRPS precipitation data were used to estimate the erosivity factor. CHIRPS was chosen for its long-term data availability and relatively high spatial resolutions as compared to most other satellite rainfall products. This product has good applicability over the Horn of Africa and has been validated in Ethiopia by Dinku et al. [63]. Moreover, in ground-station data-scarce countries such as Ethiopia, CHIRPS-v.2 is good alternative for climatological studies [64]. CHIRPS precipitation at 8-day temporal resolution and 1 km spatial resolution was obtained from GEE for 42 years (1981–2021). This data set was used to generate long-term mean annual rainfall in order to derive R-factor.

2.2.2. Land cover

LULC map (Fig. 4) was generated from Landsat surface reflectance images (Landsat 8 Operational land imager (OLI) sensors). LULC classification was done for the year 2021 image in order to represent the current biophysical status and observed changes after 2010 area exclosure and ecological restoration policy of Ethiopia [24,65]. The image after 2021 is less reliable to represent biophysical changes due to the war in the north Ethiopia and the damage it might caused on the land resources.

Table 1 presents the major LULC classes identified in the study area. LULC was classified using the Random forest (RF) classification algorithm in the GEE code editor. In order to improve the classification LULC classification, axillary data such as elevation, NDVI, Tasselled Cap brightness, dryness and wetness index, NDWI, and NBI (Normalized Burning Index) were utilized.

Tasselled Cap indices are used to distinguish the presence and density of green vegetation, total reflectance, and soil moisture [66]. The accuracy evaluation (Table 2) was performed using indices including the user's accuracy (UA), producer's accuracy (PA), overall accuracy (OA), and kappa coefficient [67,68]. These accuracy indices are calculated by constructing confusion matrix using GEE syntax. The GEE inbuilt code for construction of error matrix and calculation of LULC accuracy was done following Stehman [69]. Eqs (1)–(3), presents the calculations of UA, PA, and OA, respectively;

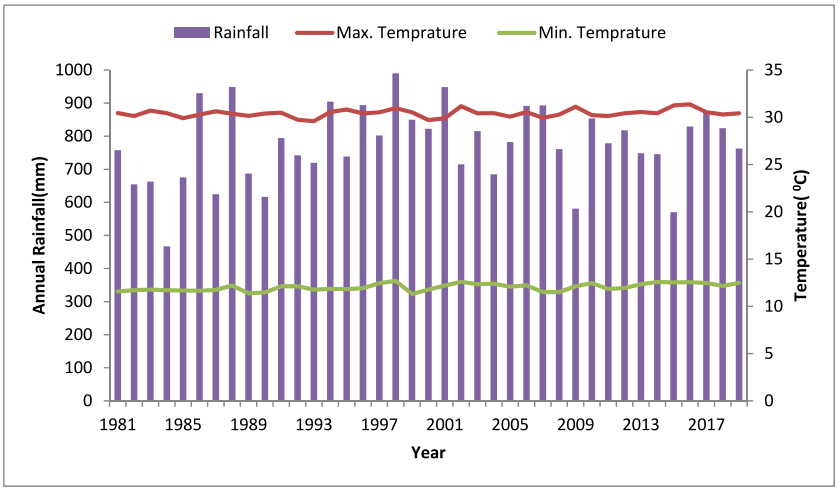

Fig. 2. Annual rainfall, minimum and maximum temperature time series in the study area from 1981 to 2021 (derived from monthly $_{\text{CHIRPS-v.2}}$).

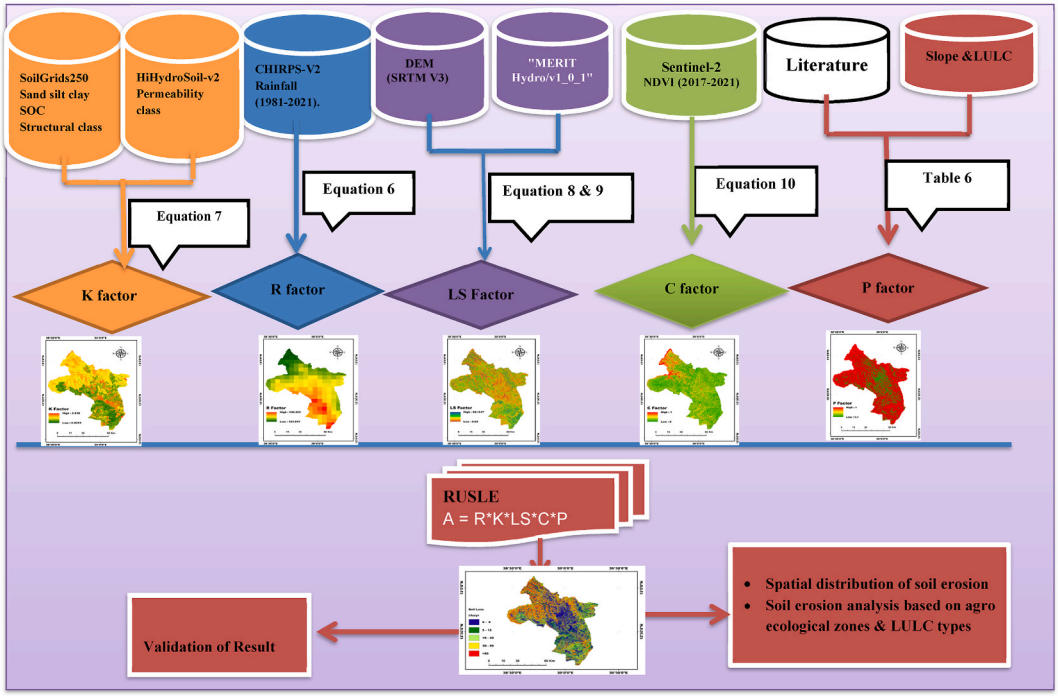

Fig. 3. Schematic presentation of the methodological framework of the study.

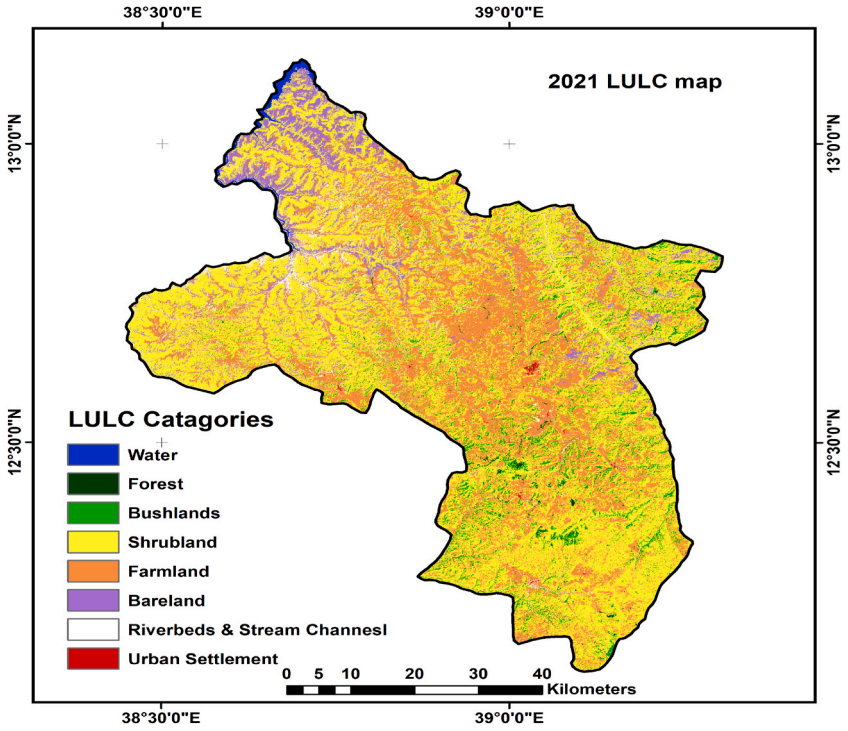

Fig. 4. Land use land cover types of Tekeze sub-basin of the Waghimra zone in Amhara region, North Ethiopia.

Table 1
Description of land use land cover classes in the study.

No	LULC classes	Description
1	(W)	An area of land covered with surface water such lakes, and rivers.
2	(F)	Areas covered by dense natural trees mainly grow naturally in the reserved land, church compounds, riverbanks, and plantations.
3	(BL)	Areas covered with small trees, woody bushes. Sparse canopy trees and dense vegetation grown in protected areas and hillsides.
4	(ShL)	Areas covered with short shrubs and bushes with little valuable wood, usually stony with a very rugged micro relief. A mix of tiny clusters of plants or single plants dispersed on open grassing land.
5	(FrL)	Cultivated land, crop fields, and fallow lands. Rural settlements fenced with trees that are commonly found around homesteads
6	(BrL)	Areas of rock or soil with very sparse to no vegetation; large areas of sand, rock, and deserts with no to little vegetation
7	(RbSc)	Dry riverbeds, stream channels, gullies, and sandy flooded areas.
8	(UrS)	The urban settlement, residential, commercial and services, industrial, and mixed-use.

Note: W = water body, F = forest, BL = bush land, Shl = shrub land, FrL = farmland, BrL = bareland, RbSc = dry river beds and stream channels, and UrS = urban settlements.

Table 2
Accuracy of the RF classification algorithm.

Year	Accuracy	LULC classes								OA	Kappa
		W	F	BL	Shl	FrL	BrL	RbSc	UrS		
2021	UA	1	0.74	0.82	0.84	0.91	0.86	0.91	1	0.88	0.82
	PA	0.93	0.81	0.85	0.86	0.90	0.91	0.89	0.82		

Note: AU = user's accuracy, PA = producer's accuracy, OA = overall accuracy, W = water body, F = forest, BL = bush land, Shl = shrub land, FrL = farmland, BrL = bareland, RbSc = dry river beds and stream channels, and UrS = urban settlements.

$$UA_i = \frac{C_{ii}}{\sum_{k=1}^{n} C_{ik}} \quad (1)$$

$$PA_J = \frac{C_{jj}}{\sum_{k=1}^{n} C_{kj}} \quad (2)$$

$$OA = \frac{\sum_{k=1}^{n} C_{kk}}{n} \quad (3)$$

Where c_{ij} = the value of the cell in row i and column j in the confusion matrix; n = the number of classes in the map.

The kappa coefficient was estimated using Eq. (4).

$$K = \frac{\sum_{i=1}^{r} x_{ii} - \sum_{i=1}^{r} x_{i+}.x_{+i}}{N^2 - \sum_{i=1}^{r} x_{i+}.x_{i+}} \quad (4)$$

Where N = total number of pixels used in the matrix, r = number of classes in the matrix, x_{ii} = correctly classified pixels in the matrix, x_{i+} = sum of pixels described in ith row, x_{+i} = sum of pixels described in ith column.

Table 2 shows the details of the accuracy evaluation of the RF classification. The classified map was obtained after the RF algorithm achieved high accuracy, 0.88 and 0.82 overall accuracy and Kappa values, respectively. The final classified map is shown in Fig. 4. This LULC map was used to identify croplands and other LULC classes for the purpose of support practice (P) factor mapping and for aggregation of erosion rate in different LULC classes.

2.2.3. Soil

The most recent and improved version of the 250 m spatial resolution SoilGrids250 m dataset developed by International Soil Reference and Information Centre (ISRIC) [70] was used for soil erodability estimation. The SoilGrids250 m data is generated based on machine-learning methods including RF, gradient boosting, and multinomial logistic regression. Geo-referenced soil profile data generated by World Soil Information Services (WSIS) have been used for the prediction of SoilGrids250 m data [70]. Previous studies have used this product for RUSLE studies [18,22,56].

2.2.4. Elevations and flow accumulation

The Shuttle Radar Topography Mission (SRTM V3) product was used for LS factors, slope, and elevation data. This dataset has 30 m

spatial resolution and undergone a void-filling process [71]. The flow accumulation (FA) area is a relatively downslope area (pixel) where all the upstream areas are draining into. We used the openly available FA dataset of MERIT Hydrograph dataset ("MERIT/Hydro/v1_0_1″) for LS factor estimation [72]. This dataset was initially generated from error-corrected and highly improved DEM. This data set has both flow accumulation pixel and flow contributing area as a distinct band and is freely available in GEE. After importing the data to the GEE code editor using ee.Image ("MERIT/Hydro/v1_0_1″) script, its resolution has been rescaled from a 90 m to a 30 m to match the SRTM V-3 30 m DEM and the LULC map. The rest of the LS components, i.e., slope and aspect, were derived from 30 m resolution SRTM V-3 available in GEE.

2.2.5. Vegetation

The NDVI for C factor was computed from a cloud-masked sentinel that has been masked for water, clouds, heavy aerosols, and cloud shadows. This product is provided at 10 m spatial resolution. We used the mean NDVI of the basin from 2017 to 2021. The baseline date is taken based on data availability of the Sentinel collection ('COPERNICUS/S2_SR').

2.3. Methods of soil loss estimation using RUSLE-GEE

Summary of data type, data source, and processing software for estimating RUSLE parameters presented in Table 3. RUSLE is an empirical model that estimates the long-term average soil loss rate by taking into account six factors that affect soil erosion: rainfall erosivity, soil erodibility, slope length and steepness, cover management, and conservation practices [38,42]. RUSLE has been very popular mainly for its easy integration with GIS. This study uses GEE, an open-source platform for analyzing geospatial data to estimate parameters of RUSLE and soil loss rates. GEE has been used worldwide for retrieving and processing earth observation data.

There is an attempt to integrate RUSLE with GEE because of the computation power of GEE and availability of geospatial data allows the estimation of RUSLE parameters. This approach is now a days mentioned as GEE-RUSLE framework [55,56]. The popular RUSLE formula is presented in Eq. (5);

$$A = R.K.LS.C.P \tag{5}$$

Where A is annual average soil loss rate (t ha^{-1} yr^{-1}) at pixel level; R is a rainfall erosivity factor (MJ mm ha^{-1} h^{-1} yr^{-1}), K is erodibility (t ha h (ha^{-1} MJ^{-1} mm^{-1})); LS factor is a dimensionless topographic factor accounting slope length (L) and slope steepness (S). C is the land cover factor, and P is a factor for erosion control support practice.

Derivation of parameters and retrieval of all the datasets were carried out in GEE (Fig. 3) and most of the model's input parameters were adjusted for the study area's specific context. The details of each parameter are presented in the following subsections.

2.3.1. Rainfall erosivity factor (R)

The rainfall erosivity factor (R) measures the power of rainfall to cause soil erosion. The major factors which cause soil erosion by causing detachment of particles are rainfall amount and intensity [43,74]. Rainfall erosivity can be calculated based on kinetic energy (E) and the maximum 30-min rainfall intensity [38,74]. Although several formulas are suggested by different researchers [75] to calculate rainfall erosivity, this study adopted Eq. (6) developed by Hurni [76], considering the Ethiopian highland arid and semi-arid region where rainfall is concentrated in a few months while the rest of the year experience deficient rainfall. Previously the equation has been used by several studies in Ethiopia [18,25,35,77].

$$R = -8.12 + 0.562(Pa) \tag{6}$$

R is rainfall erosivity in (MJ mm ha^{-1} h^{-1} yr^{-1}), and Pa is long-term mean annual rainfall (mm). We used 42 years (1981–2021) of annual rainfall for deriving the R factor.

Table 3
Summary of data type, data source, and processing software for estimating RUSLE parameters.

Parameters	Input data	Source and processing environment
R	CHIRPS-V2 rainfall data 1 km Spatial resolution for the past 42 years (1981–2021)	Obtained from GEE datasets using Javascript code ee.ImageCollection ('UCSB-CHG/CHIRPS/PENTAD')
K	SoilGrids250 m Soil organic matter, soil textural class, and soil bulk density data HiHydroSoilv2_0 [73] Permeability class, and Hydrologic group and saturated hydraulic conductivity	Filtered and computed in GEE after the data is imported from SoilGrids as (ee.Image ("projects/soilgrids-isric/–") HiHydroSoilv2_0 accessed through GEE
LS	DEM: SRTM V3 30 m resolution Flow accumulation: MERIT Hydrograph dataset	STRM DEM is freely available in GEE and imported as (ee.Image ("USGS/SRTMGL1_003″) MERIT Hydrograph dataset is available in GEE and imported as ee.Image ("MERIT/Hydro/v1_0_1″)
C	NDVI from sentinel collections	Accessed and processed in GEE
P	LULC and Slope data	Image accessed and processed in GEE

2.3.2. Soil erodibility factor (K factor)

The K-factor represents the erodability of soil particles by water. The level of resistance of soil particles to erosion is determined by the soil's physical and chemical properties, including organic matter, texture, structure, and permeability [38,42]. The significant methodological variation of RUSLE application globally comes from the presence of several equations to estimate K factor [43]. Scholars have developed different formulas to determine soil erodibility. These are mainly based on parameters such as soil grain size and the degree of saturation [78], particle size, amount of organic matter content, molecular bonding, structural class, and the rate of permeability [38,79], and soil color [76]. In this study, we applied a model that considers the particle size, organic matter, structural class, and rate of permeability developed by Wischmeier and Smith [38] and adopted by Renard et al. [42]. The formula is presented in Eq. (7).

$$\mathbf{K} = \left[\frac{\mathbf{2.1} * \mathbf{10}^{-4} * \mathbf{M}^{1.14}(\mathbf{12} - \mathbf{OM}) + \mathbf{3.25}(\mathbf{S} - \mathbf{2}) + \mathbf{3.5}(\mathbf{P} - \mathbf{3})}{\mathbf{100}}\right] * \mathbf{0.1317} \tag{7}$$

Where M is the particle size parameter and is estimated as $(\text{silt}_{\%} + \textbf{very fine sand}_{\%}) * (\mathbf{100} - \text{clay}_{\%})$, OM is the organic matter content (%), S is the soil structure code, P is the soil permeability class, and 0.1317 is a factor to convert K unit from US metric system to the international metric system unit. Not all the required data for Eq. (7) were directly available in SoilGrids250 m dataset, for example, there is no very fine sand fraction in the dataset layer, and we estimated the very fine sand fraction as 20 % of the sand fraction following Panagos et al. [7]. The upper limit of very fine sand plus silt contents was set to 70 %, and the maximum limit of OM was set to 4 % to prevent an underestimation of K values following Wischmeier and Smith [38].

2.3.3. LS factor

LS is a measure of the topographic effect in the RUSLE model. It is a function of two components, slope length (L) and slope steepness factor (S) [38,42]. Slope length is the horizontal distance from the origin of the erosion to the point where the slope gradient decrease and overland flow concentrates. S factor is also the effect of slope gradient on soil erosion by water. Different equations are available to calculate LS factor [38]. For this study, a more explained formula based on the contributing area concept has been used. In order to measure the slope length (L), the upslope contributing areas is preferred over the combined slope-length approach since the upstream area of a pixel is the key determinant factor of runoff to a given point [25,58]. The techniques of calculating L factor were given by Desmet and Govers [58] as presented in Eq. (8).

$$\boldsymbol{L_{ij}} = \frac{\left(\boldsymbol{A_{ij}} + \boldsymbol{D^2}\right)^{m+1} - \left(\boldsymbol{A_{j\,j-in}}\right)^{m+1}}{\boldsymbol{D^{m+2}} * \left(\boldsymbol{x_{ij}}^{m}\right) * \mathbf{22.13}^{m}} \tag{8}$$

where; Ai,j−in is contributing area to the grid cell (i, j) in m^2, D is the grid cell size (30 m), $\boldsymbol{X_{i,j}^{m}} = \boldsymbol{sin a_{i,j}} + \boldsymbol{cos}\ \boldsymbol{a_{i,j}}$, $\boldsymbol{a_{i,j}}$ represents the aspect of the cell (pixel).

where m (Eq. (8.1)) is related to β (Eq. (8.2)), the ratio of the rill to interill erosion suggested by Ref. [80] and later adopted by Ref. [42];

$$\boldsymbol{m} = \frac{\boldsymbol{\beta}}{\boldsymbol{\beta} + \boldsymbol{\beta}} \tag{8.1}$$

and

$$\boldsymbol{\beta} = \frac{\boldsymbol{sin}\,\boldsymbol{\beta}/\mathbf{0.896}}{\mathbf{3.0}(\boldsymbol{sin}\,\boldsymbol{\beta})^{\mathbf{0.8}} + \mathbf{0.56}} \tag{8.2}$$

Where θ is the slope angle in degrees.

In order to solve the error related to the overestimation of soil erosion in larger streams and make an ideal erosion estimate over extremely low-laying areas, we have limited the upslope contributing area to 4000 m^2 (which is almost equal to 4.5 pixels) as suggested by Zhang et al. [81]. In this study, limiting the upslope contributing area to 4000 m^2 has sustainably decreased the mean soil loss from ca. 195 to 25.5 t ha^{-1} yr^{-1}.

In order to estimate the slope steepness (S) factor, the original formula from McCool et al. [82] and later Renard et al. [42] adopted an algorithm for the S-factor estimation based on two slope gradient intervals (slope <0.09 and slope >0.09) (Eqs. (9.1) & (9.2)) as follow:

$$S = 10.8 \times \sin\theta + 0.03, \text{where slope gradient } < 0.09 \tag{9.1}$$

$$S = 16.8 \times \sin\theta - 0.5, \text{for slope gradient} \geq 0.09 \tag{9.2}$$

Where θ is the slope angle in degree.

However, due to the limitation of this method in estimating S in steeper slopes (>10°) and due to the evidence that the S-factor calculated using this method is lower by around 20 % [83,84]; we used the method of Liu et al. [83] to account for slope gradient effect greater than 10^0 (Eq. (9.3)). This S factor calculation method has been applied by previous studies (eg., Elnashar et al. [56]).

$$S = 21.91 \times \sin\theta - 0.96 \tag{9.3}$$

2.3.4. Cover management factor (C)

The cover management factor (C) represents the effects of vegetation cover on soil loss rates. The cover management factor is the dimensionless parameters of the RUSLE model. The crop cover and management factor is defined as the proportion of soil loss from land with particular vegetation [38]. C factor can be changed over time and has a significant role in soil erosion management planning. Land cover change has the most substantial influence on the C-factor, leading to a significant increase in the C-factor and soil loss. Other studies in Ethiopia used land cover as a proxy measurement for the C-factor [6,26] by assigning values from 0 in covered land surface to 1 in bareland. However, NDVI, which helps to assess the actual ground vegetation cover in every LULC type, can quickly assess the C factor [85]. Several empirical studies have proved that NDVI is a good measure of cover management factors, particularly in large-scale soil loss assessment studies [56,85]. For this study, a C-factor map of the basin was generated based on the following empirical relationship of NDVI and C factor (Eq. (10)) [86].

$$C = \exp\left(-\alpha x \frac{NDVI}{\beta - NDVI}\right) \tag{10}$$

where α and β determine the relationship between NDVI and C factors, and value of 2 and 1 was assigned for them, respectively, based on Van der Knijff et al. [86]. This method of C estimation has been used by Refs. [27,30,47,56,85]. The C factor value in this study ranges from 0 to 1. The lower C factor values represent well-protected soil, while the value approaching 1 is for bare surface.

2.3.5. Support practice factor (P)

The P in RUSLE is a human-made practice to reduce soil erosion by water and designate the effect of soil conservation and management efforts made to overcome soil erosion and runoff [6,38]. The P-factor represents the ratio of the soil loss rate in a field with a given conservation practice to the soil loss rate where no conservation practice is applied. For this study, we produced a P-factor map based on land cover, where only contour tillage on croplands was considered. In this case, P-factor values were assigned to croplands based on slope classes following the recommendation of Wischmeier and Smith [38]. In order to derive the P factor, the land cover classes are grouped into two main classes: cropland and non-cropland [25,46]. The minimum value approaching 0.1 was assigned to cropland assuming that soil and water conservation practices were applied in all croplands. For land cover types other than cropland, a P-factor value of 1 was assigned. The classification of cropland into different slope classes and assigning values (Table 4) was suggested by Ref. [38]. P values proposed for agricultural and non-agricultural landscapes were used by Refs. [12,17,56].

2.4. Validation of model results

Model validation is an important and common task in soil loss assessment studies. Validating result with field or plot based data is one and preferable validation technique, however field measured soil loss rate data is scarce in our study area for this purpose. Furthermore, comparison of our result with field or plot scale data, or with averaged soil loss rates from large geographical region may not be appropriate [87]. Due to these reasons, we followed scientific model validation by comparing our model result with previous works carried out in the study area and outside the study area. This method of model validation in soil erosion studies is commonly applied in previous studies [17,26,88,89].

3. Results and discussion

3.1. Spatial distribution of RUSLE parameters

This section discusses the spatial distribution of RUSLE parameters in the basin (Fig. 5). The parameters showed spatial variation in the study area and varying influence on the estimated soil loss rates.

R factor ranges from 353 to 535.5 MJ mm ha^{-1} h^{-1} yr^{-1} (Fig. 5A). Higher erosivity is spatially distributed in the southern and southwest part of the study area. Erosivity increases to the southern part of the basin, which it's most part is highland agroecology being the origin of most of highland streams. The erosivity ranges from 535 in the highland southern part of the basin to 354 MJ mm ha^{-1} h^{-1} yr^{-1} in the northern part (Fig. 5A). The relatively higher R-value is associated with more rainfall power to erode the soil particles and, thus, high vulnerability to erosion.

K-factor values range from 0.002315 to 0.036 t ha h (ha^{-1} MJ^{-1} mm^{-1}) (Fig. 5B). The mean K factor in the highland agroecology is

Table 4
Slope classes for assigning P value for farmlands.

Slope in percentage	P factor values
0–5	0.10
5–10	0.12
10–20	0.14
20–30	0.19
30–50	0.25
50–100	0.33

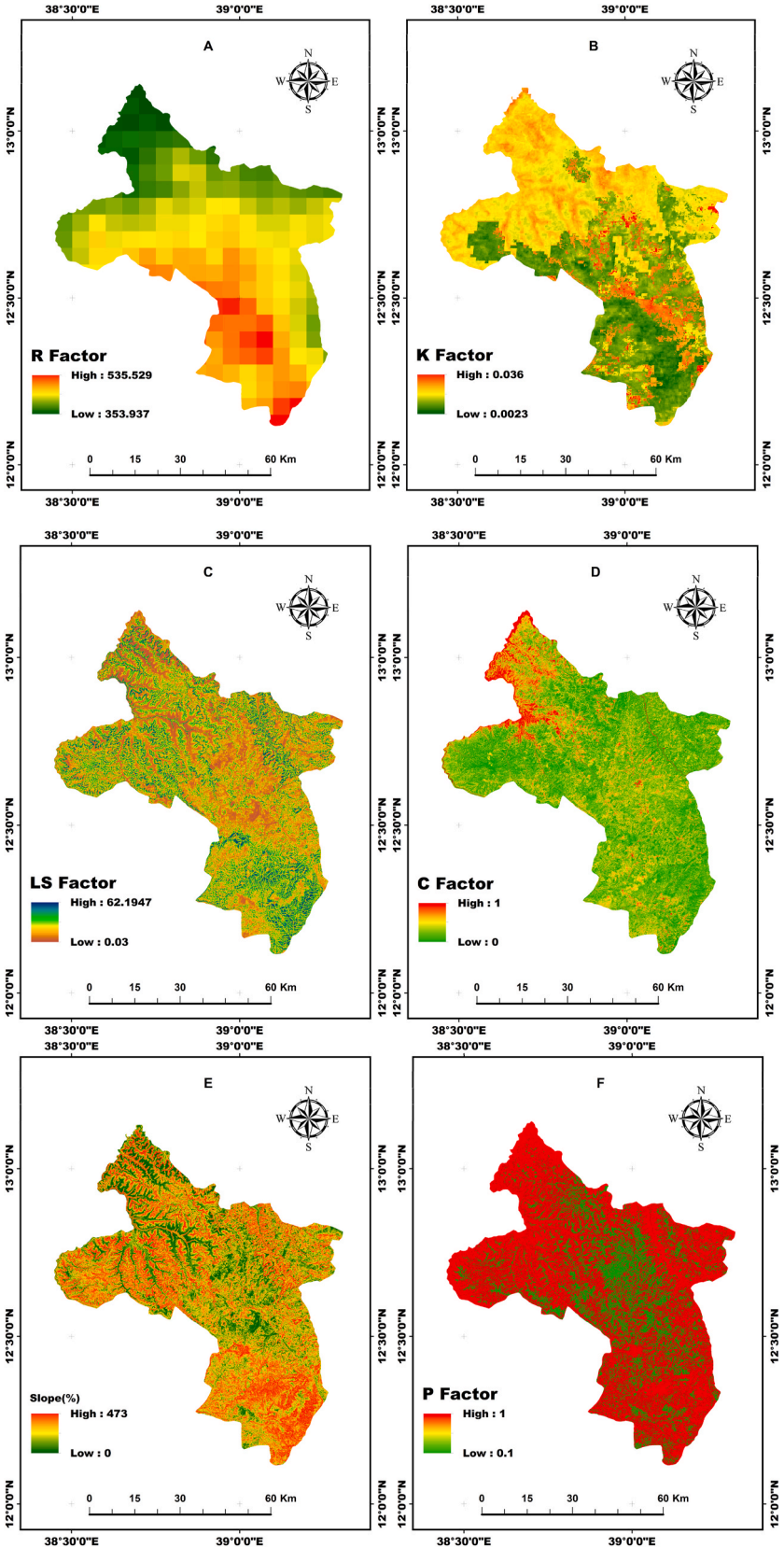

(caption on next page)

Fig. 5. Spatial distribution maps of RUSLE parameters; R factor (A), K factor (B), LS factor (C), C factor (D), Slope (E), P-factor (F).

0.00995, while it is 0.013861 and 0.017766 in the midland and lowland agroecology, respectively. The K factor distribution was the opposite of rainfall erosivity distribution. The highest K factor values were observed in the lower part of the basin, where there is a lower erosivity factor, but coincided with higher C and P factor.

The LS-factor map is shown in Fig. 5C, and ranges from 0.03 to 62.2. Higher LS factor values are located on the basin's high slope and hillside areas (Fig. 5E) both in western and eastern, and the lower and upper part of the basin. The mean LS factor is 10.013. The Dega agroecology has a higher mean LS factor of 12.34. The Weyna-dega and Kolla agroecologies have 9.3, and 8.4, respectively.

The C-factor ranges from 0 to 1 (Fig. 5D). The highest C factor values are found in the northern part of the basin where there is poor vegetation cover, eroded floodplain, and bare grounds. The lower C values are distributed in the basin's central, western, and southern parts over conserved forests and managed watersheds. These areas are relatively less vulnerable to soil erosion. Pocket areas of dense forest on less human-accessible mountainsides, church forests, and area exclosures and successful cases of integrated watershed managements were found to have lower C factor values. Generally, the C factor map (Fig. 5D) shows that the north and north-western part of the basin exhibited higher C factor values indicating lower vegetation cover. Low rainfall and aridity of rainfall contribute to the absence of vegetation cover in this part of the study area. The lower C factors are located in the southern highland of the basin. This part of the basin is where the Tekeze River and most of its tributary streams originate. In this part of the basin vegetation cover is relatively better because of relatively better annual rainfall. Despite high erodabilty factors, the area has lower C factor.

P factor is a means to measure the impact of erosion management practices on erosion rate, particularly the erosion control strategies implemented on agricultural lands. The P factor in the study area ranges from 0.1 to 1 (Fig. 5F) and the slope map that is used for classification of croplands by different slope class for the assignment of P factor values is shown on (Fig. 5E). Lower P factor is spatially distributed in the central part of the study area over the croplands. However, higher P factors area almost evenly distributed in the basin over the vast spare shrub lands and degraded wood and bush lands (Fig. 5F).

3.2. Assessment of the extent and severity of soil loss by water erosion in the upper Tekeze basin

The spatial variability of soil erosion severity rates in the upper Tekeze Basin are presented in Fig. 6. Highly eroded areas are clustered in the highland regions of the basin and over the mountainous shrub lands of the northern part of the basin mainly because of steeper slopes and higher soil erodabilty (Fig. 5B). While the rainfall erosivity is low in the northern lowland agroecology of the basin, low cover factor combined with poor management factor make the region more prone to erosion. On the other hand, a lower soil loss

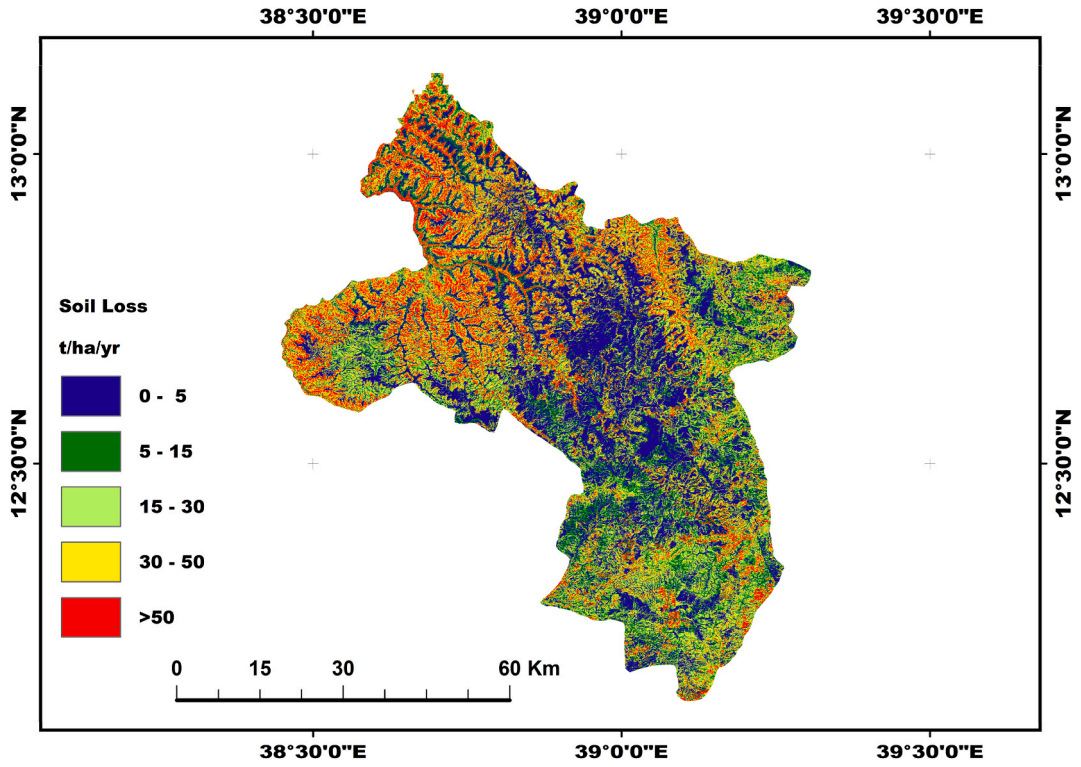

Fig. 6. Spatial distribution of soil loss rates severity in the upper Tekeze basin, (0–5; very slight), (5–15: slight), (15–30: moderate), (30–50: severe), (above 50: very sever).

rate was seen in the vast middle parts of the basin due to the lower LS factor and better cover management and support practice factors. The central midlands and the southwest part of Waghimra zone have relatively low soil erosion rate than the north and northeast part of the study area (Fig. 6).

The mean soil erosion rate in the study area is 25.46 t ha^{-1} yr^{-1}. This estimate was higher than estimates by Fentat al [87]. (16.9 t ha^{-1} yr^{-1}) for Ethiopian Basins. The result agrees with Sonneveld et al. (2011) estimate of mean soil loss rates for northwestern and central highlands of Ethiopia (more than 20 t ha^{-1} yr^{-1}). But lower than some other watershed base studies by Yirgu et al. [36] (30.6 t ha^{-1} yr^{-1}) for Upper Domba watershed in southern Ethiopia, and by Eniyew et al. [6] who reported 576 t ha^{-1} yr^{-1} for Telkwonz Watershed in northwestern Ethiopia. However, since the study was conducted over a large spatial scale, basin and sub-basin scale comparison is more appropriate and meaningful. Regarding this, the estimated mean annual soil loss rate can be considered generally consistent with estimates by Ref. [56] for the blue Nile basin in general (39.73 t ha^{-1} yr^{-1}) and lower than, estimates for upper blue Nile (57.98 t ha^{-1} yr^{-1}). Similarly, the result is in agreement with mean soil loss rates estimate by Haregeweyn et al. [16] (27.5 t ha^{-1} yr^{-1}) and Fenta et al. [22] (32.5 t ha^{-1} yr^{-1}) for upper blue Nile basin.

We have classified the soil erosion rate into five classes; less than 5 t ha^{-1} yr^{-1} (very slight), 5–15 t ha^{-1} yr^{-1} (slight), 15–30 t ha^{-1} yr^{-1} (moderate), 30–50 t ha^{-1} yr^{-1} (sever) and above 50 (very severe erosion). This classification was according to soil erosion literature in Ethiopia [16].

Areas under very slight soil loss (<5 t ha^{-1} yr^{-1}) cover 24.4 % of the basin. Slight soil loss (5–15 t ha^{-1} yr^{-1}) is also observed over for 22.5 % of the total basin area. Moderate soil loss rate is also seen in over 21.7 % of the basin. Both severe and very severe soil loss rates are observed over 31.3 % of the basin (Table 5). The very slight and slight soil loss rate classes covering 47 % of the basin contributed more than 9 % of the total soil loss. Severe and very severe soil erosion classes contributed 25 % and 47 % of the total soil loss in the basin, respectively (Table 5).

The result showed that the soil erosion severity distribution in terms of area coverage of the basin is gradually decreasing from 24.4 % very slight to 22.5 % slight, 21.7 % moderate, 16.1 % severe and then to 15.2 % very severe. However, the more significant part of the total soil loss in the basin was generated from the moderate, severe and very severe erosion classes contributing 18.25, 25.06 and 47.43 % of the total soil loss, respectively. The second and third contributors to the total soil loss are from severe and moderate soil erosion classes that cover 16.1 and 21.7 % of the basin. The severity class distribution implies that the majority of total soil loss is generated from the 15.2 % of the basin, which experiences very severe soil erosion and moderate to high erosion rates. The general pattern of the soil erosion severity distribution indicates that a high amount of soil loss rate is observed in a very large basin area. Geographically, the sight and very slight soil losses are concentrated in the middle part of the basin, with a relatively gentle slope and terraced agricultural lands. Slight erosion classes were also observed on upslope areas in highly protected watersheds (Bella-Wuleh watershed). Moderate erosions are almost evenly distributed through the basin on hilly, bare, and moderately protected area exclosures. However, the severe and very severe erosion classes are observed dominantly in the northern high-slope areas of the basin. Spares shrubs cover this part of the basin dominantly.

3.3. Soil erosion analysis viz-à-viz land cover types

The share of different LULC classes to the total soil loss in the study area is presented in Table 6. The largest share of total soil loss comes from soil erosion over shrubland, 99,950,272.9 t yr^{-1}, which counts for 79.9 % of the total soil erosion from basin. The mean annual soil loss rate from this land cover class is also the highest of all land cover (34.7 t ha^{-1} yr^{-1}). The higher soil erosion rate over shrublands could be due to the spares vegetation and higher LS factor. The LULC classification of the basin showed that most shrublands are very sparsely distributed with bare and sandy exposed surfaces. Vegetation is dry most of the year and is highly vulnerable to soil erosion during intense rainfall. This finding was consistent with [56], who reported that the highest erosion in the Blue Nile basin comes from shrublands. Low soil loss rate was found on farmland contribution being 4.25 % to the total soil loss in the study area with mean annual soil loss rate of 3.56 t ha^{-1} yr^{-1}. Mean soil loss from this study is lower than reports from studies by Fenta et al. [22,87], Yirgu [36], and Haregewoyn et al. [16]. In these studies higher mean soil loss rates were reported on cropland than other land cover types. Furthermore, reduction in cropland mean soil loss rate in this study might be due to the method applied to limit the maximum contributing area while deriving L factor. Besides, the study area is known for its ridged topography that hinders expansion of agricultural land. Furthermore, the most available agricultural land lies in the relatively gentle slope are with low annual rainfall, thus low erosivity. In most of the croplands, stone bunds are constructed to protect soil erosion. Besides, biological measures such as grasses and Aloe vera are common soil and water conservation mechanism (Fig. 7A). Due to the relatively gentle slope of farmlands and conservation structures on them, the soil erosion rate of farmlands is lower in most of the agricultural lands. However, due to the

Table 5
Soil erosion severity classes and respective total soil losses in the basin.

Severity classes (t ha^{-1} yr^{-1})	Description	Area (Km^2)	Area (%)	Mean soil loss rates (t ha^{-1} yr^{-1})	Std	Total soil loss by the class (t yr^{-1})	Contribution to the total soil loss (%)
<5	Very slight	1122	24.4	2.13	1.24	2960612.1	2.33
5–15	Slight	1033	22.5	9.60	3.0	8779632.1	6.90
15–30	Moderate	996	21.7	22.0	4.0	23159069.78	18.25
30–50	Sever	741	16.1	38.85	5.7	31,815,573.14	25.06
>50	Very severe	700	15.2	77.80	28.8	60,195,744.64	47.43

Table 6
Mean soil erosion rate and total soil loss from different LULC categories.

Land cover	Mean soil loss rates (t ha^{-1} yr^{-1})	Std	Total soil loss rate (t yr^{-1})	Contribution to the total soil loss (%)
Forests	7.2	10.4	147505.78	0.13
Bush and woodlands	22.66	19.65	5,763,929.86	4.6
Unprotected shrub lands	34.75	27.88	99,950,272.9	79.9
Farmland	3.56	7.78	5,316,081.33	4.25
Bare lands	31.68	34.46	11382931.34	9.0
Dry river beds and streams channels	27.6	28.93	2477398.37	2.0
Settlement areas	12.95	13.97	60320.578	0.05

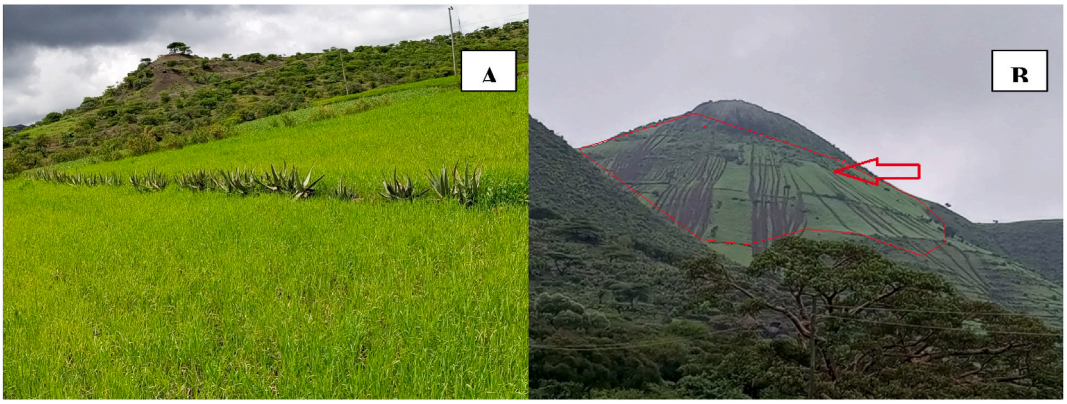

Fig. 7. Soil and water conservation mechanism implemented on croplands (A) (Aloe vera strip, Photo taken around Tiya village) and farming on steep slope areas expose to sever soil erosion (B) (Photo taken outside of Agewmariayma watershed, July 2022).

shortage of the cultivable land, some high slope areas are being converted to cropland. In these high slope areas soil erosion is extremely high. During intense rainfall, it totally damages the crops. Fig. 7B shows a photo of a mountainside newly converted to farmland. The crops are eroded by soil erosion and the soil conservation works could not withstand the force of the erosion accelerated by the slope gradient and land use conversion. Forestland is also the second that contributes lower soil erosion in the study area. Forestlands have 7.2 t ha^{-1} yr^{-1} and 0.13 % to the total soil loss in the study basin. Forests area located in the relatively high slope and elevation remote area where there is less human access. Rehabilitated watersheds with good forest cover are also found in this LULC category and contribute low soil erosion. However, bush and woodlands exposed to higher soil erosion (22.66 t ha^{-1} yr^{-1}). They are found over the complex topography and in areas with high LS factor. Most of the wood and bushlands are found in community based watershed conservation sites where exclosures are currently established. Their erosion rate is not yet reduced down to the acceptable soil erosion rate.

Bare land with a mean annual soil loss rate of 31.7 t ha^{-1} yr^{-1} contributes 9 % of total soil loss in the basin. Most of the bare lands are found in the lower part of the basin behind the Tekeze hydroelectric dam. The topography in this part of the basin is highly diverse, ranging from low deposition areas to high slop mountainsides. This area is constantly vulnerable to erosion, so soil development is challenged, and regeneration of vegetation cover is almost impossible.

3.4. Soil erosion analysis viz-à-viz agroecological zones

The agroecological classification of the Ethiopian farming system and ecosystem has great implications for soil and water conservation practice [22,60]. Soil erosion management should also consider these agroecologies since there is distinct rainfall distribution, runoff production, vegetation cover, and cropping practice. Elevation is the prime determinant of agricultural land use in Ethiopia because it influences the temperature and rainfall distribution. Generally, crop production also exhibits a distribution mosaic in Ethiopia. Some crop types are found within several zones, while others are restricted to single agroecology. This distinct crop distribution also has different runoff production, erosion vulnerability, and management requirements. In the study area, we classified

Table 7
Agroecological distribution of soil erosion risks in the upper Tekeze Basin.

Agroecology	Altitude (m)	Area (km^2)	Area (%)	Mean soil loss rate (t ha^{-1} yr^{-1})	Total soil loss rate (t yr^{-1})
Dega (Highlands)	Above 2300	668	14.54	19.8	28137689.82
Weyna-dega (Midland)	1500- 2300	3125	68	24.3	85877094.56
Kolla (Lowland)	below 1500	799	17.5	37.6	28137689.82

the agroecology into three dominant agroecological zones. While the majority of the basin is Weyna-dega (midland) and Kolla (lowland), small portion is found in Dega (highland) agroecology (Table 7).

Most of the basin (68 %) is characterized by midland (Weyna-dega) agroecology. This is the part of the basin where the most extensive cropland is found. As seen in Table 7, the mean soil loss in this agroecology is 24.3 t ha^{-1} yr^{-1}. The Weyna-dega agroecology experienced higher mean soil loss rate than the high land agroecology. The Dega agroecology is the high slope area and the origin of the major Tekeze River and its tributaries, so one might expect higher soil loss in this zone. However, this agroecology has good vegetation cover and low soil erodabilty. The Kolla (lowland) agroecology, which covers 17.5 % of the basin, experienced 37.6 t ha^{-1} yr^{-1} soil loss rate. This zone is characterized by high aridity, complex topography, and low rainfall. High K factor values, low vegetation cover characterize this agroecology.

3.5. Evaluation of model results by comparing with other assessments

This result of the RUSLE–GEE estimate of soil erosion was compared with findings of previous studies in Ethiopia, mainly in the Tekeze basin and the Upper Blue Nile River Basin. The mean soil erosion rate from this study (25.5 t ha^{-1} yr^{-1}) is comparable with other studies in the Ethiopian highlands by Sinshaw et al. [30] (25.52 t ha^{-1} yr^{-1}); and by Haregeweyn et al. [16] (27.5 t ha^{-1} yr^{-1}). Unlike these comparable reports, as presented in Table 8, higher estimates were also reported by some studies in different parts in Ethiopian highlands. For example, Elnashar et al. [56] estimated 57.98 t ha^{-1} yr^{-1} erosion rate for the upper Blue Nile basin; Ewunetu et al. [18] estimated 46 t ha^{-1} yr^{-1} for North Gojjam sub-basin of Upper Blue Nile River; and Tamene et al. [25] estimated 45 t ha^{-1} yr^{-1} in Adikenafiz, Gerebmihiz and Laelaywukro watersheds in Nothern Ethiopia. Lower estimation of mean soil loss was also reported by Kebede et al. [26] (9.1 t ha^{-1} yr^{-1}), and Ayalew [90] (13.2 t ha^{-1} yr^{-1}) for Zingin (Blue Nile) and upper Beles in the Blue Nile basin, respectively.

Besides the difference in land use management, difference in methods of estimation and datasets could result in different model results. Since the estimation was carried out in the GEE platform, different equations, and dataset for LS factor and C factor, the estimated soil loss rate is reasonable and comparable with results of previous studies, particularly with GEE-RUSLE framework and basin and sub-basin studies. Variations in time, space, assessment scales, input data, and methods followed could lead to difference in results. This is because erosion is a process with significant variation in time and space [13].

A recent review of soil erosion assessment studies in Ethiopia by Tamene et al. [91] reported that the soil loss rate in Ethiopia varies between 0 and 220 t ha^{-1} yr^{-1}, and the national average gross soil erosion rate is estimated to be 38 t ha^{-1} yr^{-1}. Studies implementing RUSLE give the highest soil loss (51 t ha^{-1} yr^{-1}), while the field-survey approach gives the lowest (20 t ha^{-1} yr^{-1}). Compared with this report, the current study estimated 25.5 t ha^{-1} yr^{-1}, slightly higher but close to the field survey approach but lower than the country average estimation using RUSLE.

However, our result is highly comparable and within the average soil erosion rate range in the sub-moist (23.6 $\pm$ 2.7 t ha^{-1} yr^{-1}) and the arid zone (28.8 $\pm$ 6.5 t ha^{-1} yr^{-1}) of Ethiopia. More importantly, the estimate from this study is highly in agreement with field experiment-based soil erosion rate in the Agewmariayam watersheds, in the current basin. Girmay et al. [92] estimated the mean soil loss rate at 25.00 t ha^{-1} yr^{-1} in Agewmariayam watershed. According to this comparison, we can say that our estimation of soil erosion rate using GEE-frame work produces reasonable results that can be used as input for land and water conservation policies.

3.6. Erosion hotspot areas for management interventions in soil erosion reduction

This study will benefit policymakers in exploring the extent and severity of soil erosion and identify hotspot areas of soil erosion in the upper basin of the Tekeze River in the Waghimra administrative zone. The spatial pattern of the soil erosion risk map (Fig. 6) shows that the entire basin experience from very slight to very severe erosion. However, because conservation efforts are economically expensive, it is impossible and economically inefficient to implement conservation measures in all areas that are affected by erosion. One of the aims of soil erosion assessment is to identify erosion hotspot areas and prioritize immediate conservation [16,22]. The soil erosion severity analysis in this study indicated that about 36.9 % of the basin is within the acceptable soil loss tolerance. Soil loss

Table 8
Comparison of the estimated mean soil loss rates by this study (25.5 t ha^{-1} yr^{-1}) with previous studies conducted in different basins in Ethiopia.

No	Basin/watershed	Slope & topographic characteristics	Dominant LULC	Mean soil loss rates (t ha^{-1} yr^{-1})	References
1	Rib Watershed	Dominated by gentle slope	Cultivated & grasslands	25.52	[30]
2	Zingin (Blue Nile)	Moderate slope	Cultivated	9.1	[90]
3	Beshillo (Blue Nile)	Dominated by high slope terrain (>30 %)	Farmland & grasslands	37	[89]
4	Upper beles (Blue Nile Basin)	flat to very steep slope	Cultivated & Bushlands	13.2	[26]
5	Upper Blue Nile Basin	Moderate slope	Cultivated land	27.5	[16]
6	Adikenafiz, Gerebmihiz & Laelaywukro	About 12^{o} mean slope	Cultivated & grazing land	45	[25]
7	Upper Blue Nile Basins	From low to high slope	Dominated by Shrub and cultivated	57.98	[56]
8	North Gojjam sub-basin (Upper Blue Nile)	Gentle to moderate slope	Cultivated land & settlement	46	[18]

tolerance is the maximum tolerable soil erosion rate that that will allows crop productivity to be sustained and does not significantly affect land productivity [38,76]. The tolerable mean annual soil loss of 10 t ha^{-1} yr^{-1} was used to evaluate the potential risk of soil erosion in the basin following previous studies in the highland of Ethiopia and the Blue Nile River basin (e.g., Refs. [22,56,87,92]). According to this threshold, 36.9 % of the study area affected is exposed to mean annual soil erosion of less than 10 t ha^{-1} yr^{-1} which can be considered as acceptable soil erosion rate. The remaining 63 % of the study area, which is affected by moderate, severe, and very severe erosion, is above the tolerable soil erosion rate, contributing 90.74 % of the total soil erosion, and hence needs an immediate soil conservation measure in order to halt this severe and very severe erosion rate. The very severe soil erosion rate alone, which covers 15.2 % of the basin, contributes 47.43 % to the total soil loss. This area is very critical and a hotspot of very severe erosion in the basin. Therefore, land management intervention should prioritize this area to reduce severe erosion. Moderate and severe erosion contribute 18.25 and 25.06 % of soil loss, respectively. The government and any natural resource conservation stakeholder, including policy-makers, should immediately consider these hotspot areas for soil conservation measures.

Over the past two decades, watershed management practices such as the construction of stone bunds and the establishment of exclosures have been implemented in the semi-arid highlands of northern Ethiopia to reduce soil erosion [93]. Regarding the effectiveness of the implemented conservation measures, studies in the highland of Ethiopia reported that physical, biological and integrated conservation measures are very effective [94,95]. In the northern highlands of Ethiopia, there is ample evidence that land management measures such as stone bunds, soil trenches, check dams afforestation, and areas exclosures are effective practices for controlling runoff and soil erosion [22,96]. For example, Taye et al. [97] showed that stone bunds, trenches, and stone bunds with trenches in rangeland and cropland are successful protection measures. Similarly, Ebabu et al. [98] demonstrated that soil bunds, combined with grass enclosure with trenches effectively reducing soil loss and runoff in the Upper Blue Nile Basin. Fenta et al. [22] reported that land cover and agroecology-specific land management practices such as level bunds, graded bunds, trenches, and exclosures could reduce the national mean soil loss rate by about 68 %. A study in north-west part of Ethiopia [99] reported that implementing conservation practices such as contour ploughing with terracing could reduce the mean annual soil erosion by 62 %.

For the identified erosion hotspot areas in the study area, suitable land management practices, including soil or stone bunds and exclosures should be implemented to minimize soil erosion. Mainly focus should be made on the vast shrublands vulnerable to natural and human-made degradation. Soil and water conservation practices have been implemented in Waghimra administrative zone for the last two decades. However, the effectiveness of these interventions varies from place to place. Substantial portion of the shrublands are open to human and animal intervention, hence vulnerable to degradation and overgrazing. Combined with the frequent drought and surface aridity, vegetation cover is unable to regenerate and protect soil from erosion. Despite challenges that hinder the effectiveness of soil conservation measures, few watersheds that achieve soil erosion under a tolerable threshold show how erosion management could be possible in the upper Tekeze basin. To compare and investigate the role of conservation measures in reducing soil erosion rate, we purposely selected four sub-watersheds in the basin and studied the mean soil erosion rate. We compared shrub land where there are poor erosion-controlling efforts with the managed watersheds and shrublands (Table 9 & Fig. 8A–D). The four examples of sub-watersheds are featured as follows: Bella-Wuleh (Fig. 8B) is under exclosure and integrated watershed management; Hamuset-Chochorba (Fig. 8C) is under soil and water conservation (SWC) practices; Asketeam (Fig. 8D) is under area exclosure; while Ziquala shrubland (Fig. 8A) is unprotected. All areas are found in relatively similar topographic settings. Mean soil erosion rate in the unprotected shrubland is about 54.58 t ha^{-1} yr^{-1}. The most successful case in soil erosion management is Bella-Wuleh watershed, showing erosion rate of 7.5 t ha^{-1} yr^{-1}. This management practice has reduced the soil erosion rate by 86.3 % from that of unprotected shrubland. In this watershed, previous study by Gebrernichael et al. [94] has confirmed that watershed management has positively transformed the upland of Bella-wuleh watershed; evidence of increase in vegetation and water has been observed after implementation of integrated watershed management. High, low, and moderate slopes characterize the area and are an upslope area susceptible to soil erosion. However, due to the continuous effort of soil and land management, the mean soil loss has dropped to 7.5 t ha^{-1} yr^{-1} (Table 9 & Fig. 8A), which is within the range of an acceptable soil erosion rate. Similarly, in the Asketema area exclosure of mountain area, protection of the area from animal grazing and human use alone has reduced the soil erosion compared with unprotected areas. The mean soil loss is reduced to 10 t ha^{-1} yr^{-1}, and is less than it's nearby unprotected mountain ridges.

Recent study by Fenta et al. [22] showed that implementation of land cover and agroecology specific management practices in the upper Blue Nile and Tekeze basin would reduce total soil loss by 50 %. Furthermore, managing erosion-prone areas in Dega and Weyna-dega agroecologies can lead to 70 % total soil loss reduction. Watershed-scale studies in northern Tekeze basin demonstrated that implementation of soil/stone bunds and exclosures reduced soil loss [93,100]. According to these empirical evidences and the observed erosion rate reduction over area exclosure and managed watersheds, it is clear that soil erosion reduction is possible if proper management and conservation is implemented on properly identified erosion hotspot areas. Soil and water conservation structures on previously degraded shrub lands have been implemented in the study area (Fig. 9A). It is evident that promising results have been obtained in protecting the soil loss and helping vegetation regeneration (Fig. 9B).

3.7. Limitation of the study

Validation of the model estimation in this study is carried out by comparing it with previous studies conducted in the highlands of Ethiopia. While such validation is common and possible in the literature, using measured soil loss data to validate the soil erosion rate would have been more appropriate. Furthermore, we could not get spatially comparable prior studies in the area to triangulate with the current study; the result was compared to the studies conducted by different scholars on other sub-basin of the Blue Nile in Ethiopia. In addition, this estimates form this study are on the annual time scale; however, future studies are needed on soil erosion estimation on seasonal and monthly time scales in order to identify the risk of soil erosion in the rainy seasons, as the rainfall is highly

Table 9
Comparison of protected and unprotected watersheds in terms of soil erosion rate.

Sampled sub-watersheds	Conservation level	Dominant LULC	Agroecology	Mean slope (%)	Mean soil loss rate (t ha^{-1} yr^{-1})
Bella-Wuleh sub-watershed	Area exclosure & Integrated watershed management	Cultivated & woodland	Weyna-dega	25.18	7.5
Hamuset- chochorba	Area exclosure with SWC practice	Shurbland	Weyna-dega	45.73	17.2
Asketeam -area closure	Area exclosure	Wood & bushland	Dega	65.65	10
Ziquala shrubland	Unprotected	Shurbland	Kolla/ Lowland	53.64	54.6

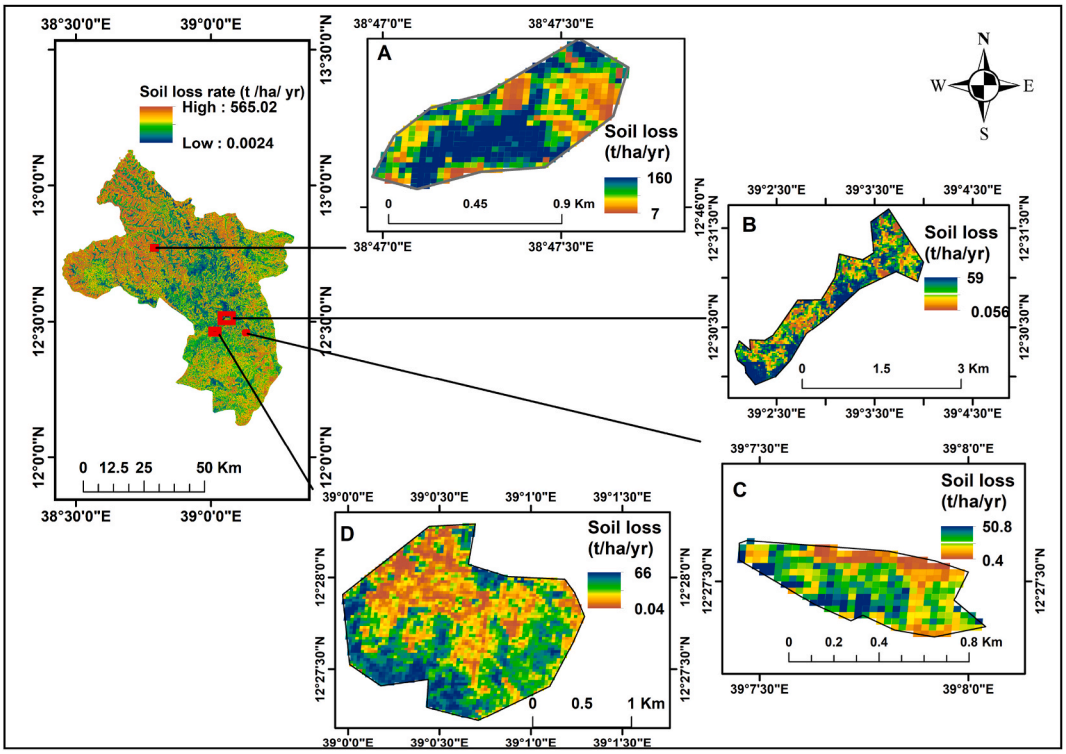

Fig. 8. Location of the sample sub watershed in the study area and their soil loss rates (t ha^{-1} yr^{-1}) (A: Ziquala shrubland, B: Bella Wuleh sub-watershed, C: Hamuset-Chochorba, D: Asketema area exclosure).

Fig. 9. Soil and water conservation structure on degraded shrub lands (A: Stone bund on previously degraded shrubland, and B: Soil retention and vegetation growth along the constructed stone bunds).

unevenly concentrated on the three (June, July, August) months in the basin. Finally, since RUSLE-GEE depend on free and open data sources, error also might arise from the lack of a very fine sand layer in the SoilGrids250 m dataset. Due to the absence of very fine sand data in the SoilGrids250 m dataset, we used very fine sand as 20 % of the sand fraction, as suggested by Ref. [7]. Finding an alternative data source or adding the very fine sand layer to the SoilGrids250 m dataset is necessary for future studies to improve the estimation of soil erosion rate in GEE.

4. Conclusions

As soil resource is increasingly vital with the growing food demand of the increasing world population, a practical soil erosion assessment framework is desired for conservation and management practices. This study assesses soil erosion by water using the RUSLE model in the GEE platform in the Upper Tekeze basin in Waghimra administrative zone, one of the oldest settlement areas of Northern Ethiopia. This study used all required data from GEE freely available datasets. Besides, all the computation and analysis of the RUSLE parameter and the final soil erosion statistics were performed inside GEE code editor. Our RUSLE-GEE model estimates 25.5 t ha^{-1} yr^{-1} mean annual soil loss rate in the study area. On about 1939.5 km^2 (36.9 %) area of the Upper Tekeze Basin rate of soil loss by erosion is with an acceptable soil erosion rates below 10 t ha^{-1} yr^{-1}, whereas about 63 % of the area showed above acceptable rates, ranging from 10 to over 50 t ha^{-1} yr^{-1}. Soil loss analysis by land cover type demonstrated that the highest soil loss rates are found in sparsely vegetated shrub lands; contributing about 80 % of the total soil loss of the basin. Both in terms of mean soil loss rate and contribution to the total soil loss, bare lands are the second most erosion hotspot areas in the Upper Tekeze basin. Croplands have significantly lower mean erosion rate of 3.56 t ha^{-1} yr^{-1} and contribute a lower percentage (4.25 %) to the total soil loss of the basin. The result showed that about 63 % of the study area requires immediate soil conservation measures. Particularly, the focus should be given to shrublands that have the highest mean soil erosion rate and significant contribution to the total soil erosion rate in the study area. Wood and bush lands located in high slope area are also among the highest vulnerable LULC classes to soil erosions that need soil and water conservation measures. Area exclosures and adoption of different soil erosion controlling mechanisms such as terracing, and stone and soil bonds on exposed shrublands have good reputability in minimizing soil erosion in the highlands of Ethiopia. Few watersheds in the study area that achieve soil erosion within the tolerable threshold show how erosion management could be possible in the climatologically harsh and topographically complex region of upper Tekeze basin. We compared shrub land where there are poor erosion-controlling efforts with the managed watersheds and shrub lands. Mean soil erosion in the unprotected shrubland was found being the highest, about 54.58 t ha^{-1} yr^{-1}. However, on managed watershed, due to the continuous effort of soil and land management, the mean soil loss has dropped within the range of the acceptable soil erosion rate. Area exclosure from animal grazing and human use has reduced the soil loss rates. Therefore, this study concludes watershed management using area exclosure and soil and water conservation practices can help to reduce soil erosion and to rehabilitate and protect the ecosystem, and also to protect croplands from sever erosion.

The study also highlighted that using RF algorism has improved land cover classification for RUSLE model; using freely available datasets in the GEE, SoilGrids250 m, and high-resolution sentinel images in GEE are the greatest benefits of GEE-RUSLE framework for soil erosion studies.

Funding statement

This research did not receive any specific grant from funding agencies in the public, commercial, or not-for-profit sectors.

Data availability statement

Data used in this study will be available on request.

CRediT authorship contribution statement

Alemu Eshetu Fentaw: Writing – review & editing, Writing – original draft, Methodology, Formal analysis, Data curation, Conceptualization. **Assefa Abegaz:** Writing – review & editing, Supervision, Methodology, Conceptualization.

Declaration of competing interest

The authors declare that they have no known competing financial interests or personal relationships that could have appeared to influence the work reported in this paper.

Acknowledgement

We would like to acknowledge Addis Ababa University for providing financial assistance to Alemu Eshetu for data collection. We also would like to thank United States Geological Survey (USGS) and GEE developer team for providing data and computation capacities in GEE. Finally, we thank field assistances and farmers in the study area for giving us their time and support during fieldwork.

References

[1] A. Arneth, F. Denton, F. Agus, A. Elbehri, K. Erb, B.O. Elasha, M. Rahimi, M. Rounsevell, A. Spence, R. Valentini, Framing and context, in: Climate Change and Land: an IPCC Special Report on Climate Change, Desertification, Land Degradation, Sustainable Land Management, Food Security, and Greenhouse Gas Fluxes in Terrestrial Ecosystems, 2019.

[2] M.S. Reed, M. Buenemann, J. Atlhopheng, M. Akhtar-Schuster, F. Bachmann, G. Bastin, H. Bigas, R. Chanda, A.J. Dougill, W. Essahli, A.C. Evely, L. Fleskens, N. Geeson, J.H. Glass, R. Hessel, J. Holden, A.A.R. Ioris, B. Kruger, H.P. Liniger, W. Mphinyane, D. Nainggolan, J. Perkins, C.M. Raymond, C.J. Ritsema, G. Schwilch, R. Sebego, M. Seely, L.C. Stringer, R. Thomas, S. Twomlow, S. Verzandvoort, Cross-scale monitoring and assessment of land degradation and sustainable land management: a methodological framework for knowledge management, Land Degrad. Dev. 22 (2011) 261–271, https://doi.org/10.1002/ldr.1087.

[3] M.S. Reed, L.C. Stringer, A.J. Dougill, J.S. Perkins, J.R. Atlhopheng, K. Mulale, N. Favretto, Reorienting land degradation towards sustainable land management: linking sustainable livelihoods with ecosystem services in rangeland systems, J. Environ. Manag. 151 (2015) 472–485, https://doi.org/10.1016/j.jenvman.2014.11.010.

[4] IPBES, The IPBES assessment report on land degradation and restoration, Montanarella, L. Scholes, R. Brainich, A, Bonn, Germany (2018), https://doi.org/10.4324/9781315640051-105.

[5] R. Pandit, J.A. Parrotta, A.K. Chaudhary, D.L. Karlen, D.L.M. Vieira, Y. Anker, R. Chen, J. Morris, J. Harris, P. Ntshotsho, A framework to evaluate land degradation and restoration responses for improved planning and decision-making, Ecosyst. People 16 (2020) 1–18, https://doi.org/10.1080/26395916.2019.1697756.

[6] S. Eniyew, M. Teshome, E. Sisay, T. Bezabih, Integrating RUSLE model with remote sensing and GIS for evaluation soil erosion in Telkwonz Watershed, Northwestern Ethiopia, Remote Sens. Appl. Soc. Environ. 24 (2021) 100623, https://doi.org/10.1016/j.rsase.2021.100623.

[7] P. Panagos, K. Christos, B. Cristiano, G. Ioannis, Seasonal monitoring of soil erosion at regional scale : an application of the G2 model in Crete focusing on agricultural land uses, Int. J. Appl. Earth Obs. Geoinf. 27 (2014) 147–155, https://doi.org/10.1016/j.jag.2013.09.012.

[8] E.A. Abdelsamie, M.A. Abdellatif, F.O. Hassan, A.A. El Baroudy, E.S. Mohamed, D.E. Kucher, M.S. Shokr, Integration of RUSLE model, remote sensing and GIS techniques for assessing soil erosion Hazards in arid zones, Agric. For. 13 (2023) 1–19, https://doi.org/10.3390/agriculture13010035.

[9] L. Volkova, S.H. Roxburgh, N.C. Surawski, P. C, Mick Meyer, C.J. Weston, Improving reporting of national greenhouse gas emissions from forest fires for emission reduction benefits: an example from Australia, Environ. Sci. Pol. 94 (2019) 49–62, https://doi.org/10.1016/j.envsci.2018.12.023.

[10] R.M. Doherty, S. Sitch, B. Smith, S.L. Lewis, P.K. Thornton, Implications of future climate and atmospheric CO2 content for regional biogeochemistry, biogeography and ecosystem services across East Africa, Glob. Chang. Biol. 16 (2010) 617–640, https://doi.org/10.1111/j.1365-2486.2009.01997.x.

[11] S. Eriksen, K. O'Brien, L. Rosentrater, Climate Change in Eastern and Southern Africa, 2008, p. 27.

[12] A.A. Fenta, A. Tsunekawa, N. Haregeweyn, J. Poesen, M. Tsubo, P. Borrelli, P. Panagos, M. Vanmaercke, Land susceptibility to water and wind erosion risks in the East Africa region, Sci. Total Environ. (2019) 135016, https://doi.org/10.1016/j.scitotenv.2019.135016.

[13] N. Haregeweyn, A. Tsunekawa, J. Nyssen, J. Poesen, M. Tsubo, D. Tsegaye Meshesha, B. Schütt, E. Adgo, F. Tegegne, Soil erosion and conservation in Ethiopia: a review, Prog. Phys. Geogr. 39 (2015) 750–774, https://doi.org/10.1177/0309133315598725.

[14] H. Hurni, S. Abate, A. Bantider, B. Debele, E. Ludi, B. Portner, B. Yitaferu, Z. Gete, Analysing degradation and rehabilitation for sustainable land management in the highlands of Ethiopia, Land Degrad. Dev. 9 (2010) 529–542, https://doi.org/10.1002/(SICI)1099-145X(199811/12)9:6<529::AID-LDR313>3.0.CO;2-O.

[15] H. Hurni, Degradation and conservation of the resources in the Ethiopian highlands, Mt. Res. Dev. 8 (1988) 123–130, https://doi.org/10.2307/3673438.

[16] N. Haregeweyn, A. Tsunekawa, J. Poesen, M. Tsubo, D.T. Meshesha, A.A. Fenta, J. Nyssen, E. Adgo, Comprehensive assessment of soil erosion risk for better land use planning in river basins: case study of the Upper Blue Nile River, Sci. Total Environ. 574 (2017) 95–108, https://doi.org/10.1016/j.scitotenv.2016.09.019.

[17] M. Mathewos, M. Tsegaye, N. Wondrade, Soil erosion variations along land use and land cover dynamics in Matenchose watershed, Rift Valley Basin, Southern Ethiopia, Nat. Resour. Model. (2023), https://doi.org/10.1111/nrm.12379.

[18] A. Ewunetu, B. Simane, E. Teferi, B.F. Zaitchik, Mapping and quantifying comprehensive land degradation status using spatial multicriteria evaluation technique in the headwaters area of upper blue nile river, Sustain. Times 13 (2021) 1–28, https://doi.org/10.3390/su13042244.

[19] A. Negese, E. Fekadu, H. Getnet, Potential soil loss estimation and erosion-prone area prioritization using RUSLE, GIS, and remote sensing in chereti watershed, northeastern Ethiopia, Air Soil. Water Res. 14 (2021), https://doi.org/10.1177/1178622120985814.

[20] S. Gebreselassie, O.K. Kirui, A. Mirzabaev, Economics of land degradation and improvement in Ethiopia, in: N. E, , et al.L. Econ (Eds.), Degrad. Improv. - A Glob. Assess. Sustain. Dev., 2015, pp. 401–430, https://doi.org/10.1007/978-3-319-19168-3_14.

[21] I. Niang, O.C. Ruppel, M.A. Abdrabo, A. Essel, C. Lennard, J. Padgham, P. Urquhart, Africa: Climate Change 2014: Impacts, Adaptation, and Vulnerability (2014), https://doi.org/10.1017/CBO9781107415386.002.

[22] A.A. Fenta, A. Tsunekawa, N. Haregeweyn, M. Tsubo, H. Yasuda, T. Kawai, K. Ebabu, M.L. Berihun, A.S. Belay, D. Sultan, Agroecology-based soil erosion assessment for better conservation planning in Ethiopian river basins, Environ. Res. 195 (2021) 110786, https://doi.org/10.1016/j.envres.2021.110786.

[23] FDRE, Ethiopia's Climate- Resilient Green Economy Strategy Agriculture(CRGE), FDRE, 2011. http://www.uncsd2012.org/content/documents/287CRGEEthiopiaGreenEconomy_Brochure.pdf.

[24] MoFED, Growth and transformation plan of Ethiopia (GTP), 2010/2011- 2014/15 of the federal democratic republic of Ethiopia (FDRE), Minist. Financ. Econ. Dev. 1 (2010) 14–120. https://www.greengrowthknowledge.org/national-documents/ethiopia-growth-and-transformation-plan-i.

[25] L. Tamene, Z. Adimassu, E. Aynekulu, T. Yaekob, Estimating landscape susceptibility to soil erosion using a GIS-based approach in Northern Ethiopia, Int. Soil Water Conserv. Res. 5 (2017) 221–230, https://doi.org/10.1016/j.iswcr.2017.05.002.

[26] Y.S. Kebede, N.T. Endalamaw, B.G. Sinshaw, H.B. Atinkut, Modeling soil erosion using RUSLE and GIS at watershed level in the upper beles, Ethiopia, Environ. Challenges 2 (2021), https://doi.org/10.1016/j.envc.2020.100009.

[27] V.N. Balabathina, R.P. Raju, W. Mulualem, G. Tadele, Estimation of soil loss using remote sensing and GIS-based universal soil loss equation in northern catchment of Lake Tana Sub-basin, Upper Blue Nile Basin, Northwest Ethiopia, Environ. Syst. Res. 9 (2020), https://doi.org/10.1186/s40068-020-00203-3.

[28] T.A. Duguma, Soil erosion risk assessment and treatment priority classification: a case study on guder watersheds, Abay river basin, Oromia, Ethiopia, Heliyon 8 (2022) 100174, https://doi.org/10.1016/j.heliyon.2022.e10183.

[29] T. Getnet, A. Mulu, Assessment of soil erosion rate and hotspot areas using RUSLE and multi-criteria evaluation technique at Jedeb watershed, Upper Blue Nile, Amhara Region, Ethiopia, Environ. Challenges 4 (2021) 100174, https://doi.org/10.1016/j.envc.2021.100174.

[30] B.G. Sinshaw, A.M. Belete, B.M. Mekonen, T.G. Wubetu, T.L. Anley, W.D. Alamneh, H.B. Atinkut, A.A. Gelaye, T. Bilkew, A.K. Tefera, A.B. Dessie, H.M. Fenta, A.M. Beyene, B.B. Bizuneh, H.T. Alem, D.G. Eshete, S.B. Atanaw, M.A. Tebkew, M. Mossie Birhanu, Watershed-based soil erosion and sediment yield modeling in the Rib watershed of the Upper Blue Nile Basin, Ethiopia, Energy Nexus 3 (2021) 100023, https://doi.org/10.1016/j.nexus.2021.100023.

[31] H. Liu, W. Zhao, Y. Liu, Assessment on the soil retention service of water erosion in the Nile river basin considering vegetation factor variance from 1982 to 2013, Water (Switzerland) 12 (2020), https://doi.org/10.3390/w12072018.

[32] M. Dananto, A.O. Aga, P. Yohannes, L. Shura, Assessing the water-resources potential and soil erosion hotspot areas for sustainable land management in the gidabo watershed, Rift Valley lake basin of Ethiopia, Sustain. Times 14 (2022), https://doi.org/10.3390/su14095262.

[33] C. Tamire, E. Elias, M. Argaw, Spatiotemporal dynamics of soil loss and sediment export in upper bilate river catchment (UBRC), central Rift Valley of Ethiopia, Heliyon 8 (2022) 100174, https://doi.org/10.1016/j.heliyon.2022.e11220.

[34] G. Taye, T. Teklesilassie, D. Teka, H. Kassa, Assessment of soil erosion hazard and its relation to land use land cover changes : case study from alage watershed , central Rift Valley of Ethiopia, Heliyon 9 (2023) e18648, https://doi.org/10.1016/j.heliyon.2023.e18648.

[35] B. Wolde, A. Moges, R. Grima, Assessment of the combined effects of land use/land cover and climate change on soil erosion in the Sile watershed, Ethiopian Rift Valley Lakes Basin, Cogent Food Agric. 9 (2023), https://doi.org/10.1080/23311932.2023.2273630.

[36] T. Yirgu, Assessment of soil erosion hazard and factors affecting farmers' adoption of soil and water management measure: a case study from Upper Domba Watershed, Southern Ethiopia, Heliyon 8 (2022) 100174, https://doi.org/10.1016/j.heliyon.2022.e09536.
[37] C.G. Karydas, P. Panagos, I.Z. Gitas, A classification of water erosion models according to their geospatial characteristics, Int. J. Digit, Earth 7 (2014) 229–250, https://doi.org/10.1080/17538947.2012.671380.
[38] W.H. Wischmeier, D.D. Smith, Predicting Rainfall Erosion Losses: a Guide to Conservation Planning, Department of Agriculture, Science and Education Administration, 1978.
[39] J.R. Williams, H.D. Berndt, Sediment yield prediction based on watershed hydrology, Trans. ASAE (Am. Soc. Agric. Eng.) 20 (1977) 1100–1104, https://doi.org/10.13031/2013.35710.
[40] R.P.C. Morgan, J.N. Quinton, R.E. Smith, G. Govers, J.W.A. Poesen, K. Auerswald, G. Chisci, D. Torri, M.E. Styczen, The European soil erosion model (eurosem): a dynamic approach for predicting sediment transport from fileds and small catchments, Earth Surf. Process. Landforms 23 (1998) 527–544.
[41] D.C. Flanagan, J.R. Frankenberger, C.S. Renschler, J.M. Laflen, B.A. Engel, Simulating small watersheds with water erosion prediction Project technology, in: M.J.C. Ascough II, D.C. Flanagan, St Joseph (Eds.), Soil Eros. Res. 21st Century, Proc. Int. Symp., ASABE, Honolulu, HI, USA, 2001, https://doi.org/10.13031/2013.3282.
[42] K.G. Renard, G.R. Foster, G.A. Weesies, D.K. McCool, D. Yoder, Predicting Soil Erosion by Water: a Guid to Conservation Planning with Revised Universal Soil Loss Equarion(RUSLE), 1997.
[43] P. Borrelli Panagos, K. Meusburger, B. Yu, A. Klik, K.J. Lim, J.E. Yang, J. Ni, C. Miao, N. Chattopadhyay, S.H. Sadeghi, Z. Hazbavi, M. Zabihi, G.A. Larionov, S. F. Krasnov, A.V. Gorobets, Y. Levi, G. Erpul, C. Birkel, N. Hoyos, V. Naipal, P.T.S. Oliveira, C.A. Bonilla, M. Meddi, W. Nel, H. Al Dashti, M. Boni, N. Diodato, K. Van Oost, M. Nearing, C. Ballabio, Global rainfall erosivity assessment based on high-temporal resolution rainfall records, Sci. Rep. 7 (2017) 1–12, https://doi.org/10.1038/s41598-017-04282-8.
[44] P. Panagos, P. Borrelli, K. Meusburger, C. Alewell, E. Lugato, L. Montanarella, Estimating the soil erosion cover-management factor at the European scale, Land Use Pol. 48 (2015) 38–50, https://doi.org/10.1016/j.landusepol.2015.05.021.
[45] A.A. Ugese, J.O. Ajiboye, E.S. Ibrahim, E.N. Gajere, A. Itse, H.A. Shaba, Soil loss estimation using remote sensing and RUSLE model in koromi-federe catchment area of jos-east LGA , plateau state , Nigeria, Geomatics 2 (2022) 499–517, https://doi.org/10.3390/geomatics2040027.
[46] C.G. Karydas, P. Panagos, The G2 erosion model: an algorithm for month-time step assessments, Environ. Res. 161 (2018) 256–267, https://doi.org/10.1016/j.envres.2017.11.010.
[47] A. Hagras, Estimating water erosion in the EL-Mador Valley Basin, South-West Matrouh City, Egypt, using revised universal soil loss equation (RUSLE) model through GIS, Environ. Earth Sci. 82 (2023) 1–17, https://doi.org/10.1007/s12665-022-10722-0.
[48] N. Gorelick, M. Hancher, M. Dixon, S. Ilyushchenko, D. Thau, R. Moore, Google earth engine: planetary-scale geospatial analysis for everyone, Remote Sens. Environ. 202 (2017) 18–27, https://doi.org/10.1016/j.rse.2017.06.031.
[49] L. Kumar, O. Mutanga, Google Earth Engine applications since inception: usage, trends, and potential, Rem. Sens. 10 (2018) 1–15, https://doi.org/10.3390/rs10101509.
[50] N. Sazib, I. Mladenova, J. Bolten, Leveraging the google earth engine for drought assessment using global soil moisture data, Rem. Sens. 10 (2018), https://doi.org/10.3390/rs10081265.
[51] A.E. Fentaw, A.A. Yimer, G.A. Zeleke, Monitoring spatio-temporal drought dynamics using multiple indices in the dry land of the upper Tekeze Basin, Ethiopia, Environ. Challenges 13 (2023) 100781, https://doi.org/10.1016/j.envc.2023.100781.
[52] Y.H. Tsai, D. Stow, H.L. Chen, R. Lewison, L. An, L. Shi, Mapping vegetation and land use types in Fanjingshan National Nature Reserve using google earth engine, Rem. Sens. 10 (2018), https://doi.org/10.3390/rs10060927.
[53] S. Wu, X. Gao, J. Lei, N. Zhou, Y. Wang, Spatial and temporal changes in the normalized difference vegetation index and their driving factors in the desert/grassland biome transition zone of the Sahel region of Africa, Rem. Sens. 12 (2020) 1–27, https://doi.org/10.3390/rs12244119.
[54] M. Aghababaei, A. Ebrahimi, A.A. Naghipour, E. Asadi, J. Verrelst, Vegetation types mapping using multi-temporal landsat images in the google earth engine platform, Rem. Sens. 13 (2021) 1–15, https://doi.org/10.3390/rs13224683.
[55] M. Petito, S. Cantalamessa, G. Pagnani, F. Degiorgio, B. Parisse, M. Pisante, Impact of conservation agriculture on soil erosion in the annual cropland of the apulia region (southern Italy) based on the RUSLE-GIS-GEE framework, Agronomy 12 (2022), https://doi.org/10.3390/agronomy12020281.
[56] A. Elnashar, H. Zeng, B. Wu, A.A. Fenta, M. Nabil, R. Duerler, Soil erosion assessment in the Blue Nile Basin driven by a novel RUSLE-GEE framework, Sci. Total Environ. 793 (2021) 148466, https://doi.org/10.1016/j.scitotenv.2021.148466.
[57] H. Wang, H. Zhao, Dynamic changes of soil erosion in the taohe river basin using the RUSLE model and google earth engine, Water (Switzerland) 12 (2020), https://doi.org/10.3390/W12051293.
[58] P.J.J. Desmet, G. Govers, A GIS procedure for automatically calculating the USLE LS factor on topographically complex landscape units, J. Soil Water Conserv. 51 (1996) 427–433. https://www.jswconline.org/content/51/5/427.
[59] S. Tesfaye, G. Taye, E. Birhane, S. Eatm, V. Der Zee, Observed and model simulated twenty-first century hydro-climatic change of Journal of Hydrology : regional Studies Observed and model simulated twenty- fi rst century hydro-climatic change of Northern Ethiopia, J. Hydrol. Reg. Stud. 22 (2019) 100595, https://doi.org/10.1016/j.ejrh.2019.100595.
[60] H. Hurni, Agroecologial belts of Ethiopia: explanatory notes on three maps at a scale of 1:1,000,000, Res. Report, Soil Conserv. Res. Program, Addis Ababa (1998) 43.
[61] E. Hagos, T. Ayenew, S. Kebede, M. Alene, Review of hydrogeology of tekeze river basin : implications for rural and urban water supply in the region, Ethiop, J. Sci. 38 (2015) 91–110.
[62] K. Hermans-Neumann, J. Priess, M. Herold, Human migration, climate variability, and land degradation: hotspots of socio-ecological pressure in Ethiopia, Reg. Environ. Change 17 (2017) 1479–1492, https://doi.org/10.1007/s10113-017-1108-6.
[63] T. Dinku, C. Funk, P. Peterson, R. Maidment, T. Tadesse, Validation of the CHIRPS satellite rainfall estimates over eastern Africa, R. Meteorol. Soc. 144 (2018) 292–312, https://doi.org/10.1002/qj.3244.
[64] D.A. Mariano, C.A.C. do Santos, B.D. Wardlow, M.C. Anderson, A.V. Schiltmeyer, T. Tadesse, M.D. Svoboda, Use of remote sensing indicators to assess effects of drought and human-induced land degradation on ecosystem health in Northeastern Brazil, Remote Sens. Environ. 213 (2018) 129–143, https://doi.org/10.1016/j.rse.2018.04.048.
[65] W. Mekuria, M. Wondie, T. Amare, A. Wubet, T. Feyisa, B. Yitaferu, Restoration of degraded landscapes for ecosystem services in North-Western Ethiopia, Heliyon 4 (2018) 100174, https://doi.org/10.1016/j.heliyon.2018.e00764.
[66] L. Qu, Z. Chen, M. Li, J. Zhi, H. Wang, Accuracy improvements to pixel-based and object-based LULC classification with auxiliary datasets from google earth engine, Rem. Sens. 13 (2021), https://doi.org/10.3390/rs13030453.
[67] C.C. Fonte, L. See, M. Lesiv, S. Fritz, L.D. Dinis, Assessing the accuracy of land use land cover (lulc) maps using class proportions in the reference data, ISPRS Ann. Photogramm. Remote Sens. Spat. Inf. Sci. 3 (2020) 669–674.
[68] J. Sharma, R. Prasad, V.N. Mishra, V.P. Yadav, R. Bala, Land use and land cover classification of multispectral landsat-8 satellite imagery using discrete wavelet transform, Int. Arch. Photogramm. Remote Sens. Spat. Inf. Sci. XLII–5 (2018) 703–706, https://doi.org/10.5194/isprs-archives-xlii-5-703-2018.
[69] S. V Stehman, Selecting and interpreting measures of thematic classification accuracy, Remote SENS. ENVIHON. 62 (1997) 77–89.
[70] T. Hengl, J.M. De Jesus, G.B.M. Heuvelink, M.R. Gonzalez, M. Kilibarda, A. Blagotić, W. Shangguan, M.N. Wright, X. Geng, B. Bauer-Marschallinger, M. A. Guevara, R. Vargas, R.A. MacMillan, N.H. Batjes, J.G.B. Leenaars, E. Ribeiro, I. Wheeler, S. Mantel, B. Kempen, SoilGrids250m: Global Gridded Soil Information Based on Machine Learning, 2017, https://doi.org/10.1371/journal.pone.0169748.
[71] D.A. Farr, G. Tom, Paul A. Rosen, Edward Caro, Robert Crippen, Duren Riley, Hensley Scott, Michael Kobrick, Mimi Paller, Ernesto Rodriguez, Ladislav Roth, David Seal, Scott Shaffer, Joanne Shimada, Jeffrey Umland, Marian Werner, Michael Oskin, Douglas Burbank, The Shuttle radar topography mission, Rev. Geophys. 45 (2007) 880–881, https://doi.org/10.1029/2005RG000183.

[72] D. Yamazaki, D. Ikeshima, J. Sosa, P.D. Bates, G.H. Allen, T.M. Pavelsky, MERIT hydro: a high-resolution global hydrography map based on latest topography dataset, Water Resour. Res. 55 (2019) 5053–5073, https://doi.org/10.1029/2019WR024873.
[73] G. Simons, R. Koster, P. Droogers, Hihydrosoil v2. 0-high resolution soil maps of global hydraulic properties. Future Works, 2020 [online] Available from, https://www.futurewater.eu/projects/hihydrosoil.
[74] W.H. Wischmeier, D.D. Smith, Rainfall energy and its relationship to soil loss, Eos, Trans. Am. Geophys. Union 39 (1958) 285–291, https://doi.org/10.1029/TR039i002p00285.
[75] K. Ghosal, S. Das Bhattacharya, A review of RUSLE model, J. Indian Soc. Remote Sens. 48 (2020) 689–707, https://doi.org/10.1007/s12524-019-01097-0.
[76] H. Hurni, Erosion–productivity–conservation systems in Ethiopia, in: IV Int. Conf. Soil Conserv. Novemb. 3-9, 1985 Maracay, Venez, 1985, pp. 654–674.
[77] T.B. Tadesse, S.A. Tefera, Comparing potential risk of soil erosion using RUSLE and MCDA techniques in Central Ethiopia, Model. Earth Syst. Environ. 7 (2021) 1713–1725, https://doi.org/10.1007/s40808-020-00881-z.
[78] E.W. Dangler, S.A. El-Swaify, Erosion of selected Hawaii soils by simulated rainfall, Soil Sci. Soc. Am. J. 40 (1976) 769–773, https://doi.org/10.2136/sssaj1976.03615995004000050040x.
[79] G.R. Foster, D.K. McCool, K.G. Renard, W.C. Moldenhauer, Conversion of the universal soil loss equation to SI metric units, J. Soil Water Conserv. 36 (1981) 355 LP–359. http://www.jswconline.org/content/36/6/355.abstract.
[80] Foster, L.D. Meyer, C.A. Onstad, Erosion equation derived from basic erosion principles, Trans. Am. Soc. Agric. Eng. 20 (1977) 678–682, https://doi.org/10.13031/2013.35627.
[81] H. Zhang, J. Wei, Q. Yang, J.E.M. Baartman, L. Gai, X. Yang, S.Q. Li, J. Yu, C.J. Ritsema, V. Geissen, An improved method for calculating slope length (λ) and the LS parameters of the Revised Universal Soil Loss Equation for large watersheds, Geoderma 308 (2017) 36–45, https://doi.org/10.1016/j.geoderma.2017.08.006.
[82] D.K. McCool, L.C. Brown, G.R. Foster, C.K. Mutchler, L.D. Meyer, Revised slope steepness factor for the universal soil loss equation, Trans. Am. Soc. Agric. Eng. 30 (1987) 1387–1396, https://doi.org/10.13031/2013.30576.
[83] B. Liu, K. Zhang, Y. Xie, An empirical soil loss equation, in: 12th ISCO Conf, 2002, pp. 21–25.
[84] P. Panagos, P. Borrelli, K. Meusburger, A new European slope length and steepness factor (LS-factor) for modeling soil erosion by water, Geosci. 5 (2015) 117–126, https://doi.org/10.3390/geosciences5020117.
[85] G. Thakuriah, GIS-based revised universal soil loss equation for estimating annual soil erosion: a case of lower Kulsi basin, India, SN Appl. Sci. 5 (2023), https://doi.org/10.1007/s42452-023-05303-0.
[86] J.M. Van der Knijff, R.R.J.a. Jones, L. Montanarella, Soil erosion risk assessment in Italy, Eur. Soil Bur. (2000). https://esdac.jrc.ec.europa.eu/ESDB_Archive/serae/GRIMM/italia/eritaly.pdf.
[87] A.A. Fenta, A. Tsunekawa, N. Haregeweyn, J. Poesen, M. Tsubo, P. Borrelli, P. Panagos, M. Vanmaercke, J. Broeckx, H. Yasuda, T. Kawai, Y. Kurosaki, Land susceptibility to water and wind erosion risks in the East Africa region, Sci. Total Environ. 703 (2020), https://doi.org/10.1016/j.scitotenv.2019.135016.
[88] T. Gashaw, A.W. Worqlul, Y.T. Dile, S. Addisu, A. Bantider, G. Zeleke, Evaluating potential impacts of land management practices on soil erosion in the Gilgel Abay watershed, upper Blue Nile basin, Heliyon 6 (2020) 100174, https://doi.org/10.1016/j.heliyon.2020.e04777.
[89] A.Y. Yesuph, A.B. Dagnew, Soil erosion mapping and severity analysis based on RUSLE model and local perception in the Beshillo Catchment of the Blue Nile Basin, Ethiopia, Environ. Syst. Res. 8 (2019) 1–21, https://doi.org/10.1186/s40068-019-0145-1.
[90] G. Ayalew, A geographic information system based soil loss and sediment estimation in Zingin watershed for conservation planning, highlands of Ethiopia, Int. J. Sci. Technol. Soc. 3 (2015) 28, https://doi.org/10.11648/j.ijsts.20150301.14.
[91] L. Tamene, W. Abera, B. Demissie, G. Desta, K. Woldearegay, K. Mekonnen, Soil erosion assessment in Ethiopia: a review, J. Soil Water Conserv. 2 (2022), https://doi.org/10.2489/jswc.2022.00002.
[92] G. Girmay, A. Moges, A. Muluneh, Estimation of soil loss rate using the USLE model for Agewmariayam Watershed , northern, Agric. Food Secur. (2020) 1–12, https://doi.org/10.1186/s40066-020-00262-w.
[93] A.A. Fenta, H. Yasuda, K. Shimizu, N. Haregeweyn, A. Negussie, Dynamics of soil erosion as influenced by watershed management practices: a case study of the agula watershed in the semi-arid highlands of northern Ethiopia, Environ. Manage. 58 (2016) 889–905, https://doi.org/10.1007/s00267-016-0757-4.
[94] D. Gebrernichael, J. Nyssen, J. Poesen, J. Deckers, M. Haile, G. Govers, J. Moeyersons, Effectiveness of stone bunds in controlling soil erosion on cropland in the Tigray Highlands, northern Ethiopia, Soil Use Manag. 21 (2005) 287–297, https://doi.org/10.1111/j.1475-2743.2005.tb00401.x.
[95] J. Nyssen, G. Simegn, N. Taha, An upland farming system under transformation: proximate causes of land use change in Bela-Welleh catchment (Wag, Northern Ethiopian Highlands), Soil Tillage Res. 103 (2009) 231–238, https://doi.org/10.1016/j.still.2008.05.020.
[96] K. Teka, M. Haftu, M. Ostwald, C. Cederberg, Can integrated watershed management reduce soil erosion and improve livelihoods? A study from northern Ethiopia, Int. Soil Water Conserv. Res. 8 (2020) 266–276, https://doi.org/10.1016/j.iswcr.2020.06.007.
[97] G. Taye, M. Vanmaercke, J. Poesen, B. Van Wesemael, S. Tesfaye, D. Teka, J. Nyssen, J. Deckers, N. Haregeweyn, Determining RUSLE P- and C-factors for stone bunds and trenches in rangeland and cropland, North Ethiopia, Land Degrad. Dev. 29 (2018) 812–824, https://doi.org/10.1002/ldr.2814.
[98] K. Ebabu, A. Tsunekawa, N. Haregeweyn, E. Adgo, D.T. Meshesha, D. Aklog, T. Masunaga, M. Tsubo, D. Sultan, A.A. Fenta, Effects of land use and sustainable land management practices on runoff and soil loss in the Upper Blue Nile basin, Ethiopia, Sci. Total Environ. 648 (2019) 1462–1475.
[99] M. Mustefa, F. Fufa, W. Takala, GIS estimation of annual average soil loss rate from Hangar River watershed using RUSLE, J. Water Clim. Chang. 11 (2020) 529–539, https://doi.org/10.2166/wcc.2019.181.
[100] J. Nyssen, J. Poesen, J. Deckers, Land degradation and soil and water conservation in tropical highlands, Soil Tillage Res. 103 (2009) 197–202, https://doi.org/10.1016/j.still.2008.08.002.